Drosophila host defense mechanisms against filamentous fungal pathogens with diverse lifestyles

Guiqing Liu[1,2*], Yao Tian[1], Mark Austin Hanson[3], Prince Kumar Sah[1], Jun Li[2], Bruno Lemaitre[1*]

1 Global Health Institute, School of Life Science, École Polytechnique Fédérale de Lausanne (EPFL), Lausanne, Switzerland.

2 Guangdong Key Laboratory of Animal Conservation and Resource Utilization, Institute of Zoology, Guangdong Academy of Sciences, Guangzhou, China.

3 Centre for Ecology and Conservation, Faculty of Environment, Science, and Economy, University of Exeter, Penryn, United Kingdom.

*Correspondence: guiqing.liu@foxmail.com; bruno.lemaitre@epfl.ch.

Abstract

Entomopathogenic fungi serve as powerful regulators of insect populations in nature. However, how immune effectors combat fungal pathogens remains incompletely understood. We employ *Drosophila melanogaster* as a genetically tractable model to dissect immune defense mechanisms against diverse fungal pathogens. We show that the Toll pathway is the key determinant of immunity against all species tested regardless of their ecological strategy, primarily through resistance mechanisms that limit fungal proliferation. In addition, melanization, but not phagocytosis or the Imd pathway, also has a role in limiting fungal entry and proliferation. Additionally, we show that fungal protease detection by Persephone has a quantitatively more critical role than the glucan sensor GNBP3 in the activation of the Toll pathway upon fungal infection. Our study also reveals that the fly-obligate fungus *Entomophthora muscae* employs a vegetative development strategy to hide from the host immune response. These findings reveal that *Drosophila* immune mechanisms effectively defend against a broad range of fungal pathogens, while highlighting striking adaptations to overcome these defenses in highly specialized fungal pathogens such as *E. muscae.*

Introduction

Fungal infections are widespread in nature and exert a profound impact across a wide range of organisms, including agriculturally significant plants, insects, and humans (Brown, 2023; Dean et al., 2012; Wang and Wang, 2017). Interactions between fungal pathogens and their hosts are highly dynamic and intricate. This complexity arises from the vast evolutionary diversity of fungal pathogens and the ever-changing host microenvironments that influence their infection (Brown, 2023; Dean et al., 2012; Wang and Wang, 2017). An enhanced understanding of host-fungus interactions could lead to the development of more effective strategies for managing fungal infections of global importance in agriculture, public health or environmental management (Casalini et al., 2024; Rommelaere et al., 2025).

Fungal pathogens have evolved within different niches. Saprotrophic fungi such as *Cryptococcus neoformans* and *Aspergillus fumigatus* primarily inhabit the environment but have evolved independent mechanisms that facilitate animal

infections (Morelli et al., 2021; Ristow et al., 2023). In contrast, other fungal pathogens, including *Candida albicans* and entomopathogenic fungi such as *Metarhizium* and *Beauveria* species, have co-evolved with their hosts (Brown, 2023; Hu et al., 2014). Some, under strong selection to exploit their hosts for survival, have even become obligate pathogens as seen in *Entomophthora* and *Ophiocordyceps* species (Ballou et al., 2016; De Fine Licht et al., 2017; Liu et al., 2019; Wang and Wang, 2017). Unlike human-pathogenic fungi, entomopathogenic fungi can hardly grow or even survive at 37°C (Siscar-Lewin et al., 2022). The genus *Metarhizium* includes generalist species capable of infecting hundreds of insect species across various orders (e.g. *M. robertsii*, formerly classified as *M. anisopliae*) and specialist species with a narrow host range (e.g. *M. acrium* and *M. rileyi*). Comparative genomic analyses suggest that generalist species evolved from specialists by broadening their repertoire of virulence factors (Gao et al., 2011; Hu et al., 2014). Intriguingly, some specialists such as *E. muscae* and *O. unilateralis* manipulate host behavior. They prompt infected insects to climb to elevated positions, affix themselves with their proboscides, and then splay their wings before dying, thereby facilitating fungal spore dissemination (Elya et al., 2018; Hughes et al., 2011).

Entomopathogenic fungi play a crucial role in regulating insect populations in natural ecosystems. Among them, the genetics and infection biology of *Metarhizium* and *Beauveria* species have been extensively studied and several strains have been developed as environmentally sustainable mycoinsecticides (Wang and Wang, 2017). Unlike bacterial and viral pathogens, which primarily utilize oral or respiratory routes, entomopathogenic fungi primarily infect insects through direct penetration of the cuticle and proliferate within the hemolymph. As a result, they must overcome multiple defenses, including cuticular barriers and both localized and systemic immune responses (Levitin and Whiteway, 2008; Mpamhanga and Kounatidis, 2024; Westlake et al., 2024).

On the pathogen side of host-pathogen interactions, entomopathogenic fungi have evolved various virulence factors to overcome or evade host defense (Cen et al., 2017; Ma et al., 2024; Qu and Wang, 2018; Tang et al., 2025; Valero-Jiménez et al., 2016; Wang et al., 2023). Comparative genomic studies indicate that generalist fungi tend to

have an expanded repertoire of diverse protein families compared to specialist fungi, including cuticle-degrading proteins (proteases, carbohydrate esterase) and pathogen-host interaction proteins (Hu et al., 2014; Shang et al., 2016; Wichadakul et al., 2015). However, the pathogenic mechanisms of less-studied fungi, such as *M. rileyi* and *E. muscae*, as well as the host defense responses they elicit, remain largely unexplored (Boucias et al., 2016; Elya and De Fine Licht, 2021).

The fruit fly *Drosophila melanogaster* serves as a powerful model organism for investigating multiple defense mechanisms against fungal infections (Levitin and Whiteway, 2008; Mpamhanga and Kounatidis, 2024; Westlake et al., 2024). A range of immune receptors detect microbial molecules and damage-associated signals, triggering key immune responses such as the Imd and Toll pathways, phagocytosis and melanization. The Toll and Imd pathways coordinate the production of immune effectors by the fat body during systemic infection (De Gregorio, 2002; Rommelaere et al., 2024; Uttenweiler-Joseph et al., 1998; Valanne et al., 2011; Westlake et al., 2024). The Imd pathway controls the production of antibacterial peptide (e.g. Diptericin, Cecropin) and is critical to resist infection by Gram-negative bacteria (Carboni et al., 2022; Hanson et al., 2019). The Toll signaling pathway is critical to resist fungal infection and infection with Gram positive bacteria (Lemaitre et al., 1996; Ryckebusch et al., 2025). It can be activated by two mechanisms: if a key fungal cell wall component, β-1,3-glucan, binds to the secreted pattern-recognition receptor GNBP3, or if fungal proteases activate a complex extracellular cascade of serine proteases, the Toll-PO cascade. Both mechanisms converge to the activating cleavage of the Toll ligand Spätzle (Spz) (El Chamy et al., 2008; Gottar et al., 2006; Westlake et al., 2024). Binding of Spz to the Toll receptor initiates an intracellular cascade leading to the production of a battery of host defense peptides (Weber et al., 2003). Among them, genetic and *in vitro* studies have revealed the role of Drosomycin, Metchnikowin, Bomanins, Daisho and Baramicin to combat fungal infection (Clemmons et al., 2015; Cohen et al., 2020; Fehlbaum et al., 1994; Hanson et al., 2021; Levashina et al., 1995). These host defense peptides can function additively or synergistically to combat pathogens, but they can also display high specificity toward a pathogens (Hanson, 2024; Lazzaro et al., 2020). The Toll-PO cascade also activates

105 the melanization reaction. It leads to the maturation of ProPhenoloxidases (PPO) into
106 Phenoloxidases (PO) that produce melanin and reactive oxygen species with
107 antimicrobial activity (Dudzic et al., 2019; Shan et al., 2023; Westlake et al., 2024).
108 The melanization reaction and phagocytosis have been shown to contribute to
109 surviving infection, including by fungi (Binggeli et al., 2014; Feldman et al., 2019;
110 Lohse and Johnson, 2008; Quintin et al., 2013).

111 Most research on entomopathogenic fungi have focused on a few model species or
112 genera, leaving the full extent of their diversity largely unexplored. Consequently, the
113 roles of immune pathways and effectors in mediating host defense against different
114 types of fungi remain poorly understood. In this study, we use *D. melanogaster* to
115 systematically assess the roles of immune modules, pathways, and immune effectors
116 in surviving fungal infections with varying lifestyles. By employing genetically
117 engineered flies with single and multiple mutations in immune genes, we aim to
118 determine: (i) which immune pathways are crucial and whether the same pathways are
119 used against different fungal species, (ii) the relative importance of immune modules
120 depending on the infection route, (iii) whether immune pathways function
121 independently or synergistically to combat different fungi, and (iv) how antifungal
122 peptides contribute individually or collectively to host defense against fungal
123 infections.

124

125 **Results**

126 **Fungal strains, modes of infection and immune deficient mutants**

127 We aimed to determine whether differences in *Drosophila* antifungal defense could
128 be revealed by using fungal pathogens with distinct lifestyles. We selected five fungal
129 species: *Aspergillus fumigatus*, *Beauveria bassiana*, *Metarhizium anisopliae*,
130 *Metarhizium rileyi*, and *Entomophthora muscae*. *A. fumigatus* is an opportunistic
131 pathogen with limited ability to penetrate the insect cuticle, yet it is pathogenic when
132 introduced systemically (Lemaitre et al., 1996). *B. bassiana*, *M. anisopliae*, *M. rileyi,*
133 and *E. muscae* are entomopathogenic fungi capable of infecting insects through the
134 cuticle (Elya et al., 2018; Wang and Wang, 2017). While *B. bassiana* and *M.*
135 *anisopliae* have broad host ranges, *M. rileyi* predominantly infects noctuid moths with

136 a more restricted host range (Boucias et al., 2016) and *E. muscae* is a fly-obligate
137 pathogen (Edwards and De Fine Licht, 2024).
138 Spores (conidia) from *A. fumigatus, B. bassiana*, *M. anisopliae* and *M. rileyi,* can
139 be produced *in vitro*, allowing us to use two infection methods: natural (topical)
140 infection via immersion of flies in a spore suspension, and systemic infection by
141 direct pricking with a needle dipped in the spore solution. In contrast, *E. muscae*
142 spores cannot be cultured outside its host. For this species, natural infections were
143 initiated by spore shower from cadavers of previously infected individuals as
144 described previously (Edwards and De Fine Licht, 2024; Elya et al., 2018) and
145 protoplasts, which can be grown *in vitro*, were used for injections. Fly stocks were
146 maintained at 25°C, but infections were carried out at 29°C for *A. fumigatus*, *B.*
147 *bassian*a, *M. anisopliae*, and *M. rileyi,* and 21°C for *E. muscae*. The immune pathway
148 mutants and antimicrobial peptide-deficient strains used in this study have been
149 described previously (Hanson et al., 2019; Ryckebusch et al., 2025). Most mutations
150 were isogenized in w^{1118} DrosDel background by seven rounds of successive
151 backcrosses (referred to as "iso"), although some non-isogenized mutants were also
152 included in this study (see full list of genotypes in Table S1).
153
154 **Toll and melanization contribute to surviving fungal natural infections**
155 Survival analysis upon topical natural infection with the five fungi were performed
156 with male w^{1118} *Drosdel flies (hereafter wild-type flies) and* flies specifically deficient
157 for Toll (spätzle, spz^{rm7}), Imd (Relish, Rel^{E20}), phagocytosis ($NimC1^{1}$; $Eater^{1}$) and
158 melanization ($PPO1^{\Delta}$, $PPO2^{\Delta}$), as well as compound mutant flies simultaneously
159 lacking these four modules (*Hayan-*psh^{Def}; $NimC1^{1}$; $eater^{1}$, Rel^{E20} hereafter named
160 *ΔIPTM* for *ΔIMD, ΔTOLL, ΔPhag, ΔMel*) (Ryckebusch et al., 2025). Survival upon
161 natural infection reveals the major contribution of the Toll pathway, and to a lesser
162 extent melanization to host defense against these five fungal pathogens, while
163 deficiency in IMD and Phagocytosis have no significant effect (Figs. 1A-E). The
164 absence of major role of the cellular response is supported by our observation that
165 hemoless adults that have reduced number of plasmatocytes due to the overexpression
166 of *Bax* show no or only a mild susceptibility to *B. bassiana* or *M. anisopliae*,

167 respectively (Figs. S1A-D). The susceptibility of *spz*^{rm7} flies was similar to that of
168 *ΔIPTM* flies lacking all four immune modules indicating that Toll is by far the most
169 important pathway to survive all the tested fungi (Table S3). However, *ΔIPTM* flies
170 were more susceptible than *spz*^{rm7} flies to *A. fumigatus,* but this likely reflects the
171 already short lifespan of *ΔIPTM* flies (Fig. 1F), as natural infection with *A. fumigatus*
172 did not cause a strong reduction in lifespan (Ryckebusch et al., 2025). Consistent with
173 the findings in males, a similar role of the Toll pathway and melanization in surviving
174 fungal infection was also observed in females, though with a lesser role for
175 melanization in defense against *B. bassiana* in females (Figs. S2A-E).

176 The four entomopathogenic fungi were more pathogenic to *Drosophila* than the
177 opportunistic pathogen *A. fumigatus* (Figs. 1A- E), reflecting their ability to naturally
178 infect flies. Although *E. muscae* is a specialist fungus that exclusively parasitizes flies,
179 it displayed the same level of pathogenicity as generalist entomopathogenic fungi *B.*
180 *bassiana* and *M. anisopliae*, and the parasitic noctuid specialist *M. rileyi* to *spz*^{rm7} flies
181 (Compare 1E to Figs. 1A-C). We estimate the quantity of spores released from twenty
182 cadavers for 24 h infection to be around 4.3×10^3 (Fig. S2F), a much lower spore
183 concentration than the ones used for natural infection with the other four fungi.

184 Collectively, our study shows that the Toll pathway is the main host defense
185 mechanism upon natural infection with the five fungal species. Beyond the Toll
186 pathway, melanization but not the Imd pathway or phagocytosis plays an important
187 role. Interestingly, survival analysis shows the high pathogenicity of *E. muscae* to
188 *Drosophila*.

189

190 **Reduced role of melanization in host defense against fungal infection upon septic**
191 **injury**

192 Injuries allow microbes to bypass the mechanical barrier normally presented by the
193 cuticle and to directly access the nutrient-rich hemolymph. We therefore analyzed the
194 role of the four immune modules in host defense against fungal pathogens using a
195 septic injury mode of infection. It should be noted that *PPO1*$^{\Delta}$, *PPO2*$^{\Delta}$ flies showed a
196 reduced capacity to survive wounding caused by a clean injury compared with
197 wild-type *w*^{1118} flies (Fig. 2F) (Binggeli et al., 2014). Survival upon septic infection

198 with spores of *B. bassiana*, *M. anisopliae*, *M. rileyi* or *A. fumigatus* revealed faster
199 kinetics of killing as expected from the direct mode of infection that bypasses the
200 crossing of the cuticle. Consistent with the observations done using a natural mode of
201 infection, the Toll pathway was the most effective module in surviving infection by *B.*
202 *bassiana*, *M. anisopliae*, *M. rileyi* and *A. fumigatus*. Interestingly, the contribution of
203 melanization was less marked upon systemic infection compared to natural infection
204 (compare Figs. 2A-D to Figs 1A-D). These results suggest that melanization has a key
205 role early in the natural infection process, possibly by inhibiting fungi at the entry
206 sites through the deposition of melanin. Unexpectedly, we observed that Rel^{E20} flies
207 were highly susceptible to *A. fumigatus* upon septic infection (Fig. 2D, Table S3), but
208 not by natural infection (Fig. 1D, Table S3). This points to a role of the humoral Imd
209 pathway against this fungus that becomes important only if the fungus can breach the
210 cuticle.
211
212 To analyze the host defense against *E. muscae* upon systemic infection, we injected
213 protoplasts in wild-type and immune deficient flies. Faster killing by *E. muscae* was
214 observed when injected with higher concentration of protoplasts (Fig. S3F), which
215 indicates that injection of protoplasts is a valid method to initiate infection in flies.
216 Intriguingly, flies deficient for each of the four main immune modules showed similar
217 susceptibility to the wild-type flies after injection with *E. muscae* protoplasts.
218 Although *ΔIPTM* flies display a significantly increased susceptibility upon injection
219 with *E. musca* protoplasts (Fig. 2E), the difference between *ΔITPM* flies injected
220 with *E. muscae* protoplasts and clean injury was not significant (Fig. 2F, Table S3),
221 indicating this difference rather reflects the baseline response of *ΔITPM* flies to injury.
222 Similar findings were consistently observed in females (Figs. S3A-E).
223 We conclude that the mode of infection alters the importance and involvement of
224 different immune modules. Natural infection by depositing spores on the cuticle
225 requires the melanization response to some extent, while direct injection of spores
226 bypasses this melanization-mediated defense. On the other hand, the humoral Imd
227 pathway plays little to no role in defense against natural infection, but an important
228 role can be revealed specifically upon *A. fumigatus* systemic infection. We also

229 observed that injection of *E. muscae* protoplasts kills immune mutant and wild-type
230 flies with similar kinetics, despite immunity being involved in defense against natural
231 infection.
232
233 **Natural infection with *E. muscae* barely induces the Toll pathway**
234 Having revealed its contribution to combat infection with the five fungi, we next
235 monitored the activity of the Toll pathway during the natural infection using the
236 *Drosomycin* (*Drs*) as a read-out, a Toll-regulated gene coding for an antifungal
237 peptide. Natural infection with the *B. bassiana* and *M. anisopliae* triggered a
238 relatively strong expression of the Toll pathway, representing about 20-30% of the
239 level observed 24 h after systemic injury with the model, Toll-eliciting bacterium *M.*
240 *luteus* (Figs. 3A-B compared to 3F). Natural infection with *M. rileyi* triggers a
241 significant Toll pathway activity although only at the time point of 120 h, suggesting a
242 delayed activation (Fig. 3C). *A. fumigatus* did not trigger the Toll pathway within the
243 timeframe upon natural infection, where if anything, *Drs* levels were depressed (Fig.
244 3D). The low Toll pathway activation by *A. fumigatus* is likely due to the weak ability
245 of this fungus to penetrate insect by the natural route. Collectively, the level of
246 induction of the Toll pathway correlates with the level of pathogenicity using the
247 natural infection mode with *M. anisopliae>B. bassiana>M. rileyi >A. fumigatus*. In
248 sharp contrast, *E. muscae*, despite being very pathogenic to flies, triggers a low
249 induction of *Drs* expression and this upregulation of *Drs* was observed only at the 24
250 h after infection (Fig. 3E). Expression of another Toll pathway read-out, the Bomanin
251 *BomBc3*, exhibited similar expression to that of *Drs* (Figs. S4A-E). Natural infection
252 of flies carrying the *Drosomycin-GFP* (*Drs-GFP*) reporter (Ferrandon, 1998) also
253 confirmed that *B. bassiana* induced a much stronger expression of the Toll pathway
254 compared to *E. muscae* (Fig. 3G). Thus, natural infection with *E. muscae* either fails
255 to activate the Toll pathway or suppresses it.
256 To distinguish between these two alternatives, we compared the Toll pathway
257 activity of unchallenged flies and flies 48 h after natural infection with *E. muscae*
258 upon septic injury with the Gram-positive bacterium *M. luteus*, a strong inducer of the
259 Toll pathway. We found that 24 h post-infection with *M. luteus, Drs* expression was

260 similarly induced to a high level in both unchallenged flies and flies exposed to *E.*
261 *muscae* natural infection 48 h prior to *M. luteus* infection, suggesting there was no
262 ongoing suppression of Toll signaling by *E. muscae* (Fig. 3F). Use of flies carrying
263 the *Drs-GFP* reporter revealed similar kinetics of *Drs* expression in 48 h *E. muscae*
264 infected flies and unchallenged flies following infection with *M. luteus* (Fig. 3H).
265 These experiments suggest that natural infection with *E. muscae* fails to activate the
266 Toll pathway rather than suppresses it.

267 We then compared Toll pathway activity upon septic infection by a needle dipped
268 in spores of *B. bassiana,* or injection of protoplasts of *E. muscae*. As expected, the
269 direct introduction of *B. bassiana* spores triggers a strong *Drs* expression with earlier
270 kinetics compared to natural infection (Fig. 3I). In contrast, injection of *E. muscae*
271 protoplasts did not trigger the Toll pathway more than injury alone as revealed by the
272 low and similar levels of *Drs* expression in both PBS clean injury controls and
273 protoplast-injected flies (Fig. 3J). Expression of another Toll pathway read-out the
274 Bomanin *BomBc3* exhibited similar expression trend to that of *Drs* (Figs. S4F-G). Use
275 of flies carrying the *Drs-GFP* reporter after systemic infection with spores of *B.*
276 *bassiana* and protoplasts of *E. muscae* further confirmed these observations made by
277 qRT-PCR (Fig. 3K). We infer that protoplasts are not detected by Toll pathway
278 sensors and that this may provide a mechanism for *E. muscae* to proliferate in the
279 hemolymph without triggering the immune response.

280 Collectively, our study shows that natural infection with *B. bassiana*, *M. anisopliae*
281 and *M. rileyi* triggers a strong induction of the Toll pathway, consistent with their
282 pathogenicity. Despite its pathogenicity, natural infection with *E. muscae* triggers only
283 a low Toll pathway activity indicating that this fungus is not recognized by the
284 immune system.

285

286 **_Entomophthora muscae_ hides from the host immune response using a vegetative**
287 **development strategy**

288 To explore the strategies employed by *E. muscae* to hide from Toll sensing, we
289 investigated the dynamics of *E. muscae* development inside flies. We first inspected
290 the steps leading to the protoplast-hypha transition *in vitro* by analyzing protoplast

differentiation in Grace's insect media. We observed that *E. muscae* protoplasts change from a round to an irregular shape (Fig. 4A). The protoplasts grow and elongate towards both ends and other directions along the sites of vesicle of protoplast. Calcofluor White M2R staining showed the absence of cell walls of these protoplasts before their transformation to hyphae after more than two-weeks culture in the Grace's Insect Medium. We observed the presence of vesicles in both protoplasts and hyphae during the development process in Grace's insect media (red arrow in Figure 4). Vesicle-driven outward expansion of the membrane ultimately results in pinching of the fungal cell to generate "subprotoplasts". Vesicles have been demonstrated to promote infection and stimulate protective immunity, depending on the species and host context (Lai et al., 2023; Reis and Rodrigues, 2025; Rodrigues et al., 2024). In addition, DAPI staining reveals that these protoplasts are multinucleated, and in the process of elongating, nuclei disperse along the extension of the protoplasts (Fig. S5). Next, we analyzed protoplast differentiation in flies. Morphology observation of flies showed that the entire infectious process of *E. muscae* could be divided into five stages, namely, early infection stage, fungal spores contact and subsequently penetrate the host cuticle (Stage 1/S1), intra-hemolymph growth stage, protoplasts proliferate inside the flies exhibiting erect wings (S2), protoplasts transformed to invasive hyphae stage, flies affixing themselves with their proboscides just prior to death (S3), hyphal growth stage, dead flies with a swollen and white abdomen with full of hyphae in the hemocoel (S4), hyphae extrude and produce spores from the cadavers (S5) (Fig. 4B). Staining fungal cell by dissecting flies at the above stages S1-S5 with Calcofluor White M2R, which marks fungal chitin in the cell wall, reveals that protoplasts undergo differentiation to hyphae only prior to death in the later stages, with no cell wall at S1 and S2, much thinner cell walls at S3 compared to invasive hyphae at S4 and hyphae sporulating on the cadavers at S5 (Fig. 4C). Microscopic observation showed that the development of *E. muscae* protoplasts also underwent the same morphological steps in host hemocoel as observed *in vitro* (Fig. 4A to Fig. 4C). Although protoplasts undergo the same differentiation process in infected flies, the transition from protoplasts to hyphae takes place 4 to 7 days after fly infection, compared to two weeks in the Grace's Insect Medium. Thus, the formation of

322 invasive hyphae is a process that take place very late in the infection process, just
323 before fly death. The observation that injection of *E. muscae* protoplasts are not
324 recognized by the immune system, and that *E. muscae* persists in the first stage of
325 infection as protoplasts, suggests that this fungus hides from the immune system by
326 using a cell wall-less structure.
327

328 **The Persephone branch of the Toll-PO serine protease cascade is more critical**
329 **than the GNBP3 -modSP branch to activate the Toll pathway**

330 The Toll pathway is activated upon the maturation of the Toll ligand Spz by a
331 complex cascade of serine proteases called the Toll-PO serine protease (SP) cascade,
332 which also regulates the maturation of PPOs (Westlake et al., 2024). Lysine-type
333 peptidoglycans from Gram-positive bacteria and β-glucans from fungi are detected by
334 the pattern recognition receptors (PRRs) PGRP-SA (with its adaptor GNBP1) and
335 GNBP3, respectively (Gottar et al., 2006; Michel et al., 2001) This triggers the
336 sequential activation of SPs ModSP, Grass, and Psh/Hayan (Buchon et al., 2009;
337 Dudzic et al., 2019; El Chamy et al., 2008; Kambris et al., 2006). Psh and Hayan
338 mediate the activation of SPE, which cleaves Spz, which then dimerizes and binds to
339 the Toll receptor inducing an intracellular cascade leading to the production of
340 Toll-regulated effectors such as antimicrobial peptides (Jang et al., 2006; Weber et al.,
341 2003). Psh (and likely Hayan) can also be independently cleaved by microbial
342 proteases (El Chamy et al., 2008; Gottar et al., 2006; Issa et al., 2018). Hayan and Psh
343 also regulate downstream SPs that activate PPO1 and PPO2, initiating the
344 melanization response leading to cuticular blackening and microbicidal activities (Fig.
345 5A) (Dudzic et al., 2019; Nam et al., 2012; Shan et al., 2023; Westlake et al., 2024).
346 Having shown the critical role of the Toll pathway upon natural infection with
347 entomopathogenic fungi, we investigated the mechanisms that activate Toll focusing
348 on *B. bassiana*, *M. anisopliae, M. rileyi* and *E. muscae*. In these experiments, we used
349 flies carrying the *GNBP3*^{hades} null mutation over a deficiency *Df(ED4421),* as we
350 noticed that *GNBP3*^{hades} homozygous flies display a marked susceptibility to fungal
351 infection that was not observed in transheterozygote *GNBP3*^{hades}*/Df(ED4421)* flies,
352 pointing to a background effect (Figs. S6A and 6B). The marked susceptibility of the

353 *psh*^{SK1} analysis showed that Psh contributes to host defense against *B. bassiana*, *M.*
354 *anisopliae, M. rileyi* and *E. muscae* (Figs. 5B-E). In contrast, the role of the glucan
355 binding sensor GNBP3 was modest as revealed by the almost wild-type survival of
356 *GNBP3*^{hades}*/Df(ED4421)* flies to *B. bassiana*, *M. anisopliae, M. rileyi* and *E. muscae*
357 (Figs. 5B-E, Table S3). Similar results were obtained when using another recently
358 generated *GNPB3*$^{\Delta}$ deficient mutant (Lu et al., 2024) (Figs. S6A and S6B). As ModSP
359 integrates signals from GNBP3 as a PRR of the Toll-PO SP cascade (Buchon et al.,
360 2009), we expected that *modSP*^{1} flies would exhibit the same host defense as
361 *GNBP3*^{hades}*/Df (ED4421)* flies against fungal infection. We indeed observed that
362 *modSP*^{1} flies exhibited the same ability as *GNBP3/Df (ED4421)* flies to survive *B.*
363 *bassiana*, *M. anisopliae* and *M. rileyi (*Fig 5B-D). Strikingly, *modSP*^{1} flies but not
364 *GNBP3*^{hades}*/Df(ED4421)* displayed a marked susceptibility to *E. muscae* similar to
365 *spz*^{rm7} flies (Fig 5E). As expected, *psh*^{1}*;;modSP*^{1} double mutants that block both
366 modes of sensing of Toll and *Hayan-psh*^{Def} double mutants displayed susceptibility
367 similar to *spz*^{rm7} flies. To further characterize the role of the Toll sensor, we next
368 monitored Toll pathway activation upon natural infection with *M. anisopliae*. We
369 restricted our analysis to this fungal species as *M. anisopliae* strongly activates the
370 Toll pathway. The expression pattern of *Drs* and *BomBc3* in the mutants confirms the
371 main role of Psh in activation of the Toll pathway upon natural infection (Figs. 5F-G).
372 Both *Drs* and *BomBc3* expression were not induced in *psh*^{SK1} flies, *Hayan-psh*^{Def}
373 double mutant flies, or *psh*^{1}*;;modSP*^{1} double mutant flies, being comparable to *spz*^{rm7}
374 flies, consistent with their high susceptibilities to fungal infection. However, the
375 expression of the Toll pathway was not affected in *GNBP3*^{hades} homozygous flies as
376 revealed by the wild-type expression of *Drs* and *BomBc3*.
377 Our results indicate that Psh is a highly important sensor in activating the Toll
378 pathway to mediate the host defense against these fungi, while GNBP3 plays only a
379 minor role. Surprisingly, we note that ModSP plays a specific role in surviving
380 infection with *E. muscae, suggesting another role of this apical serine protease*
381 *beyond integrating GNBP3 signals.*
382
383 **The Toll pathway restricts fungal growth**

384 Having characterized the importance of the Toll pathway and the underlying
385 mechanism leading to its activation, we next explored how the Toll pathway
386 effectively combats fungal infection. Protection by the immune system can be
387 mediated via resistance mechanisms that prevent pathogen growth or via tolerance
388 mechanisms that protect the host without directly inhibiting the pathogen (Pradeu et
389 al., 2024; Soares et al., 2017). We infected flies by natural infection and quantified
390 fungal proliferation after infection. qPCR levels of *B. bassiana 18S* gDNA reveal a
391 much high fungal load at 3- and 4-days post natural infection in spz^{rm7} flies compared
392 to wild-type flies (Fig. 6A). Higher fungal loads with earlier growth kinetics were also
393 found in spz^{rm7} flies compared to wild-type flies when infected with *M. anisopliae* and
394 *E. muscae* (Figs. 6B-C). To confirm and extend these results, we used a *M. anisopliae*
395 tagged GFP strain and monitored the expression of the Green Fluorescent Protein
396 (GFP) upon septic infection in both wild-type and *spz* mutant flies. We observed a
397 much higher proportion of flies with strong GFP signals in spz^{rm7} flies compared to
398 wild-type (Fig. 6D). While *M. anisopliae* disseminated throughout the body in spz^{rm7}
399 mutant flies, the fungus was restricted to the thorax in wild-type flies at 2- and 3- days
400 post infection (Fig. 6E). In keeping with this faster dissemination, the fungi broke
401 through cuticle and extrude from the cadavers of spz^{rm7} mutant flies 2 to 4-day before
402 that of *wild-type* flies. In both wild-type and spz^{rm7} flies, fungal growth eventually
403 occurs in the cadavers across all three tagmata, including the wings and legs (Fig. S7).
404 Thus, Toll act as a resistance mechanism limiting the growth of these three
405 entomopathogenic fungi.
406
407 **Multiple host defense peptides contribute to Toll antifungal activity**
408 In the last years, several host new defense peptides controlling fungal infection
409 have been identified in *Drosophila* (Hanson et al., 2025). In addition to Drs and Mtk
410 that display antifungal activity *in vitro* (Feldman et al., 2019; Moghaddam et al.,
411 2017), genetic studies have revealed that deficiencies in *Baramicin A*, *Bomanins* (12
412 genes) and *Daisho* (2 genes) cause susceptibility to specific fungi (Clemmons et al.,
413 2015; Cohen et al., 2020; Hanson et al., 2021). The role of these immune peptides has
414 never been analyzed collectively for their role in host defense against fungi. This

415 prompted us to explore the nature of downstream Toll effectors using isogenic mutant
416 lines against entomopathogenic fungi upon natural infection. In this analysis we used
417 single null mutants in *Drosomycin* (Drs^{R1}), *Metchnikowin* (Mtk^{R1}), *Baramicin A*
418 ($BaraA^{SW1}$), *Daisho1/2* ($^{\Delta}Dso$, a short deletion removing both Daisho 1 and 2) and
419 $Bom^{\Delta 55C}$ that removes ten of the twelve *Bomanins* (Clemmons et al., 2015; Cohen et
420 al., 2020; Hanson et al., 2021, 2019). We also used previously generated compound
421 mutants including Mtk^{R1}, Drs^{R1} double mutants, $^{\Delta}$AMP10 (a fly line deleted for 10
422 AMPs including *Mtk*, *AttA/B/C/D*, *DptA/B*, *Drc*, *Def*) and $^{\Delta}$AMP14 (a fly line deleted
423 for 14AMPs similar to $^{\Delta}$AMP10 with an additional deletion of the four *Cecropin*
424 genes *CecA1/A2/B/C*) flies (Carboni et al., 2022; Hanson et al., 2019). In the
425 framework of this study, we further generated four additional compound mutants to
426 see possible additivity or synergistic action of these host defense peptides including i)
427 $BaraA^{SW1}$, $^{\Delta}Dso$; ii) Mtk^{R1}, $BaraA^{SW1}$; Drs^{R1}; iii) Mtk^{R1}, $BaraA^{SW1}$, $^{\Delta}Dso$; Drs^{R1}) and
428 iv) Mtk^{R1}, $Bom^{\Delta 55C}$; Drs^{R1}.

429 Upon natural infection by fungi, the $Bom^{\Delta 55C}$, $^{\Delta}Dso$ deletions caused marked
430 susceptibility to all four entomopathogenic fungi while single mutations in *Mtk* and
431 *Drs* had no effect against any fungus. Alone, $BaraA^{SW1}$ caused a susceptibility to only
432 two of the four fungi. This reveals the critical role of *Bomanin* and *Daisho1/2* to
433 survive fungal infection (Fig. 7A and Fig. S8). We found that flies lacking both
434 *Baramicin* and *Daisho1,2* were markedly more susceptible to infection with *B.*
435 *bassiana, M. rileyi,* and *E. muscae*, compared to $^{\Delta}Dso$ single mutant flies, while the
436 difference for *M. anisopliae* was consistent in direction, but relatively minor (Table
437 S3). We also observed that Mtk^{R1}, Drs^{R1} but not Mtk^{R1} or Drs^{R1} single mutants display
438 increased susceptibility to *M. anisopliae,* but not *B. bassiana*, *M. rileyi* and *E. muscae,*
439 *revealing an additive effect against M. anisopliae specifically*. Strikingly, Mtk^{R1},
440 $Bom^{\Delta 55C}$; Drs^{R1} showed greater susceptibility to infection compared to $Bom^{\Delta 55C}$ flies
441 for *B. bassiana, M. anisopliae,* and *M. rileyi,* but not *E. muscae*. The susceptibility of
442 Mtk^{R1}, $Bom^{\Delta 55C}$; Drs^{R1} flies was slightly but consistently less marked than spz^{rm7}
443 mutant flies across all fungi. Finally, we observed that *ΔAMP14* flies display greater
444 susceptibility compared to *ΔAMP10* flies against each fungus, pointing to a role of
445 Cecropin in host defense against fungi, consistent with *in vitro* observation (Ekengren

446 and Hultmark, 1999).

447 Taken together, we show that host defense peptides regulated by the Toll pathways,
448 notably Bomanins, Daisho1/2, BaraA, Mtk and Drs largely explain the contribution of
449 Toll to survive fungus natural infections. The strength of effect was broadly consistent
450 across fungal species, with virulent species revealing a greater resolution of
451 differential susceptibilities. Generally, we did not find evidence for a specific
452 importance of any fungus-by-gene interactions among these effectors, suggesting their
453 contributions to survival are based on their collective action in antifungal defense,
454 with some being more important than others.

455

456 **Both PPO1 and PPO2 additively contribute to host defense against fungi**

457 Having described the contribution of Toll effectors, we next analyzed how
458 melanization contributes to host defense against these entomopathogenic fungi.
459 Previous studies have shown that PPO1 and PPO2 redundantly contribute to both
460 cuticular and hemolymphatic melanization (Binggeli et al., 2014; Dudzic et al., 2019).
461 Genetic approaches have allowed us to distinguish distinct activities associated with
462 PPO1 and PPO2: cuticular melanization at the injury site is dependent on PPO1
463 activated through Hayan, while an uncharacterized microbicidal activity against
464 *Staphylococcus aureus* relies on Sp7, but not Hayan, with a major role for PPO1 and a
465 lesser but important role for PPO2 (Dudzic et al., 2019); we will note, however, that
466 there is some redundancy *in vitro* regarding the capability of these SPs to cleave
467 PPO1 and PPO2 (Shan et al., 2023). Surprisingly, compared to these roles against *S.*
468 *aureus,* we confirmed a consistent but opposite trend in the importance of *PPO1* and
469 *PPO2* in defense against natural infection by each fungus (Fig. 7B and Fig. S9).
470 *PPO2* mutants were more susceptible to all fungi compare to PPO1, although *PPO1,*
471 *PPO2* double mutants were consistently more susceptible than flies deleted for *PPO2*
472 alone (Table S3). We next tested deletions in *Hayan* (*Hayan*^{SK6}) and *Sp7* (*Sp7*^{SK6}).
473 Agreeing with a primary role of Sp7 in PPO2-mediated defense, *Sp7*^{SK6} flies were as
474 susceptible to natural infection by *B. bassiana* and *M. anisopliae* as *PPO2* mutants.
475 On the other hand, *Hayan* mutation caused no susceptibility to *B. bassiana,* but a
476 similar susceptibility to *Sp7* and *PPO2* mutants to *M. anisopliae.* No single mutation

477 caused a significant mortality against *M. rileyi.* Strikingly, *Hayan* mutation, but not
478 *Sp7*, had a comparable susceptibility to *PPO2* mutants to *E. muscae.* In all cases,
479 spz^{rm7} was the most susceptible genotype.

480 We also monitored fungal load of *B. bassiana* and *M. anisopliae* in these
481 genotypes at key time points after infection. qPCR of *B. bassiana 18S* and *M.*
482 *anisopliae Rpl32* revealed trends broadly consistent with survival curves, with higher
483 fungal loads broadly correlating to survival (Figs. 8A-B). We also infected wild-type
484 and melanization deficient flies by pricking with *M. anisopliae* GFP spores in the
485 thorax. In these experiments bypassing the cuticle, we again observed faster growth of
486 *M. anisopliae GFP* in $PPO1^{\Delta}$, $PPO2^{\Delta}$ flies revealed by stronger GFP signals and
487 higher dissemination level within the body at both 2- and 3-day post-infection
488 compared to wild-type flies (Fig. 8C). Consistent with the survival analysis, we
489 observed slightly faster growth *M. anisopliae-GFP* in *PPO2* single mutants compared
490 to *PPO1* single mutants, with a slightly earlier and stronger GFP signal also seen for
491 *Hayan* and *Sp7* deficient flies both at 48 h and 72 h after pricking compared to
492 wild-type and *PPO1* mutants (Fig. 8C).

493 Collectively, we observe a stronger role of PPO2 compared to PPO1 in defense
494 against fungi. Additionally, it reveals different requirements for Sp7 and Hayan in
495 defense against these fungal species, somewhat agreeing with previous observations
496 for the role of these serine proteases in activating PPO1 or PPO2 in defense against *S.*
497 *aureus,* although there is some additional complexity to the antifungal response. There
498 was a strong correlation between susceptibility and fungal growth in the tested
499 mutants, indicating that melanization contributes to host survival by limiting fungal
500 dissemination and growth.

501

502 **Higher Toll pathway activity in $PPO1^{\Delta}$, $PPO2^{\Delta}$ mutant**

503 Finally, we explored whether the immune susceptibility of melanization defective
504 flies might result from improper Toll activity in the absence of melanization, we
505 monitored the activation of the Toll pathway in *PPO1*, *PPO2* single and double
506 mutant flies as well as *Sp7* and *Hayan* flies. Single mutations in *PPO1*, *PPO2*, *Sp7*
507 and *Hayan* did not affect the inducibility of *Drosomycin* upon natural infection with

508 *M. anisopliae* and *B. bassiana* (Figs. S10A-B). In agreement with previous studies
509 (Binggeli et al., 2014; Ryckebusch et al., 2025), we found a trend of higher Toll
510 pathway activation in *PPO1*$^{\Delta}$, *PPO2*$^{\Delta}$ double mutant flies compared to *wild-type* flies
511 upon natural infection with these two fungal species, although *PPO* single mutants
512 showed no increased Toll activity. A higher and earlier Toll pathway activation was
513 also observed upon direct introduce of *M. anisopliae* spores in the body cavity at the
514 time points of 24 h and 48 h, but not 72 h (Fig. S10C). Interestingly, we also observed
515 a higher level of *Drs* expression in *PPO1*$^{\Delta}$, *PPO2*$^{\Delta}$ flies compared to wild-type flies
516 upon injury with a clean needle (Fig. S9C). Moreover, unchallenged *PPO1*$^{\Delta}$, *PPO2*$^{\Delta}$
517 flies tend to have higher basal expression of *Drs* compare to their wild-type
518 counterpart across each time point (Fig. S10C).

519 These findings indicate that higher Toll signaling in *PPO1*$^{\Delta}$, *PPO2*$^{\Delta}$ is not strictly
520 linked to higher fungal load, but may relate to a negative feedback loop between the
521 Toll and the melanization cascade. This negative feedback loop has been proposed
522 previously using live and heat-killed microbe injections (Binggeli et al., 2014;
523 Ryckebusch et al., 2025). Here we show this increased Toll activity is true even for
524 unchallenged and clean injury treatments, suggesting a role for PPOs in regulating
525 Toll activation even in the absence of infection.

526

527 **Discussion**

528 Host–fungal pathogen interactions are complex and serve as potent drivers of
529 evolutionary diversification (Brown, 2023; Gladieux et al., 2014; Murante and Hogan,
530 2024; Shang et al., 2016). Fungal pathogens span a broad ecological spectrum -from
531 generalists like *B. bassiana* and *M. anisopliae* with wide host ranges, to specialists
532 such as *M. rileyi*, *E. muscae*, and *O. sinensis*, to opportunistic fungi like *C. albicans*
533 and *A. fumigatus*. Despite this diversity, our understanding of how fungal pathogens
534 with distinct lifestyles interact with host immunity remains incomplete (Lu et al.,
535 2024; Murante and Hogan, 2024; Qu and Wang, 2018; Wang and Wang, 2017).

536 To address this gap, we used *D. melanogaster* fly lines deficient in specific immune
537 pathways and effectors (Hanson et al., 2023, 2019; Ryckebusch et al., 2025) to
538 systematically investigate host defense against five fungal species. Consistent with

539 earlier work (Lemaitre et al., 1996; Ryckebusch et al., 2025; Westlake et al., 2024),
540 the Toll pathway emerged as the most critical immune module for defense against all
541 tested fungi. Generalist pathogens like *B. bassiana* and *M. anisopliae*, and to a lesser
542 extent the specialist *M. rileyi*, strongly induced the Toll pathway reporter gene *Drs*
543 upon natural infection. In contrast, *E. muscae* triggered only weak activation, and *A.*
544 *fumigatus* did not induce *Drs* expression at all upon natural infection. Nevertheless,
545 Toll signaling remained essential for survival even against weak inducers, suggesting
546 that basal or low-level Toll activity is sufficient to confer protection.

547 Our findings further show that Toll pathway-mediated immunity is important not
548 only after natural infection, which involves cuticle penetration, but also after systemic
549 infections when fungal spores are introduced directly into the hemolymph. This
550 emphasizes the role of the Toll pathway in limiting fungal growth systemically.
551 Recent studies using deletions of immune effectors downstream of the Toll and Imd
552 pathways have demonstrated synergistic, additive, and pathogen-specific roles in
553 survival (Hanson et al., 2025, 2019). We show here that Bomanins and Daisho
554 peptides are essential for surviving infection by generalist and specialist
555 entomopathogenic fungi. These observations align with previous studies showing the
556 broad antifungal activity of Bomanins against *Fusarium spp.*, *B. bassiana*, *M.*
557 *anisopliae*, and yeast species (Clemmons et al., 2015; Hanson et al., 2019), and
558 Daisho peptides active against *Fusarium* species and some *Aspergillus* strains (Cohen
559 et al., 2020). In addition, Baramicin A peptides are important for defense against
560 virulent *Beauveria* and *Metarhizium* species (Hanson et al., 2021; Huang et al., 2023),
561 while an individual importance for Drosomycin and Metchnikowin was not observed
562 for any fungus tested (Hanson et al., 2021, 2019). However, the Baramicin,
563 Drosomycin, and Metchnikowin peptides each contribute to defense independently
564 from other Toll effectors, evidenced by an increased mortality of *BaraA, Dso* and *Drs,*
565 *Mtk, Bom* combinatory mutants against most fungi. Our results may help make sense
566 of previous studies showing striking single-mutant susceptibilities (Cohen et al., 2020;
567 Hanson et al., 2021), as the importance of these genes was revealed in a
568 virulence-dependent, or host susceptibility-dependent, manner – virulence and
569 susceptibility broadly measuring opposite sides of the same coin. Thus, unlike the

570 specificity observed for antibacterial peptides (Hanson et al., 2023, 2019; Unckless et
571 al., 2016), the antifungal peptides we tested appear to act in a more general fashion,
572 suggesting that they target broadly conserved fungal features. The similar
573 susceptibility profiles of *BaraA*^{SW1}, *Mtk*^{R1}, *ΔDso; Drs*^{R1} mutants to *Bom*$^{\Delta 55C}$
574 underscores the critical role of these humoral Toll-mediated effectors in antifungal
575 immunity, with additional mutations (e.g. *Mtk*^{R1}, *Bom*$^{\Delta 55C}$*; Drs*^{R1} flies) increasingly
576 approaching *spz*^{rm7} levels of susceptibility. It would be interesting to achieve the full
577 Toll effector combinatory mutant line (*BaraA*^{SW1}, *Mtk*^{R1}, *Bom*$^{\Delta 55C}$, *ΔDso; Drs*^{R1}) to
578 learn if there is any host defense mediated by *spz* beyond the contributions of these
579 five effector families.

580 As our *Bom*$^{\Delta 55C}$ and *ΔDso* deletions removed large gene clusters (10 of 12
581 Bomanins and both Daisho genes), we could not assess individual gene contributions.
582 However, recent work has identified roles for specific Bomanins such as BomT1 and
583 BomT2 in surviving *Enterococcus faecalis*, *M. robertsii*, and *A. fumigatus* ribotoxins
584 (Lou et al., 2025). Identifying the Bomanins that mediate defense against the fungi
585 tested here will be an important next step. In addition, it would be interesting to
586 confirm the precise mechanism through which Cecropins improve survival against
587 entomopathogenic fungi. While these peptides can display antifungal activity *in vitro*
588 (Ekengren, 1999). The protective effect of Cecropins could therefore rely either on a
589 direct antifungal action, or an indirect role in preventing dysbiosis, perhaps also
590 modulating the cuticle microbiota that itself protects against topical fungal infections
591 (Hong et al., 2022).

592 Unexpectedly, we did not observe a major role of the glucan sensor GNBP3 in
593 activating Toll in response to *M. anisopliae*. A recent study showed that GNBP-like3
594 (GL3) acts as a bait for the fungal effector Tge1, which can inhibit GNBP3 and so
595 suppress Toll immune activation (Lu et al., 2024); itself does not propagate Toll
596 signaling. However, our results using *ΔGL3*, *ΔGNBP3* or *GNBP3*^{hades}*/Df(ED4421)*
597 flies indicate a minor role only for this GNBP3 arm of Toll signaling in survival upon
598 *B. bassiana* and *M. anisopliae* natural infection (Fig. S6). Instead, our data support a
599 predominant role for the Persephone (Psh) branch in Toll activation, suggesting that
600 entomopathogenic fungi are primarily recognized via the proteases they secrete

601 (Gottar et al., 2006). These include serine proteases and chitinases involved in cuticle
602 degradation (Qu and Wang, 2018), to which Psh may be specifically adapted.
603 Melanization also contributed to host defense, albeit to a lesser extent than Toll
604 signaling, consistent with earlier findings (Binggeli et al., 2014; Ryckebusch et al.,
605 2025). Its reduced impact upon septic infection suggests a key role at the initial
606 cuticular breach, where melanin and ROS deposition may restrict fungal entry and
607 dissemination. This is consistent with observations in *Galleria mellonella* and
608 *Anopheles gambiae*, where melanin accumulates at fungal entry sites (Vertyporokh et
609 al., 2020; Yassine et al., 2012).
610 We show that both PPO1 and PPO2 contribute to fungal resistance. Interestingly,
611 across fungal pathogens we found PPO2 plays a more prominent role in host defense
612 compared to PPO1, even after septic injury with *M. anisopliae*. Previous studies have
613 described a major role for PPO1 in wound site melanization through the action of
614 Hayan, but also PPO1 in host defense against *S. aureus* in a Hayan-independent
615 manner, with a more minor role for PPO2 (Binggeli et al., 2014; Dudzic et al., 2019;
616 Vasanth et al., 2025). However, here using entomopathogenic fungal infections, we
617 found the opposite. Unlike the case of *S. aureus,* distinct roles for *Hayan* and *Sp7* in
618 this PPO2-mediated immune defense are less clear, perhaps reflecting an importance
619 of Sp7 in the hemolymph, and of Hayan as the PPO-converting SP at the injury site as
620 suggested by its essentiality for wound blackening (Dudzic et al., 2019); however,
621 wound site blackening requires Hayan acting through PPO1. We also observed higher
622 Toll pathway activation in *PPO1, PPO2* double mutant flies compared to wild-type
623 flies upon fungal natural infection, agreeing with previous studies (Binggeli et al.,
624 2014; Ryckebusch et al., 2025). Here we additionally show this higher Toll activation
625 upon clean injury and even in unchallenged flies. This suggests that byproducts of
626 POs somehow negatively regulate Toll activation, which include terminal reactive
627 oxygen species, but also various intermediates involving the conversion of tyrosine to
628 L-DOPA and derivatives such as dopaquinone or the production of melanin from
629 5,6-dihydroxyindole (DHI) (Westlake et al., 2024). Conversely, Dopa decarboxylase
630 converts L-DOPA to dopamine, and so the deficiency of PO activity converting
631 L-DOPA to dopaquinone could result in the inverse accumulation of dopamine, likely

632 having pleiotropic effects. Here, the higher Toll activity in *PPO1, PPO2* double
633 mutant flies suggests there is effectively negative feedback exerted by the
634 melanization pathway on the Toll pathway. It would also be interesting to know if this
635 role of melanization in Toll regulation is related to the role of both modules in the
636 wound healing response (Capilla et al., 2017; Carvalho et al., 2014).

637 The Imd pathway had minimal roles in host defense against the four
638 entomopathogenic fungi tested, except during *A. fumigatus* septic infection.
639 Interestingly, volatile organic compounds from *A. fumigatus* have been shown to be
640 toxic to Imd-deficient flies (Almaliki et al., 2023), and a previous study showed that *A.*
641 *fumigatus* virulence acted through either proliferation or secretion of toxins in a
642 Bomanin and melanization-dependent manner (Xu et al., 2023), suggesting *A.*
643 *fumigatus* deploys multiple pathogen strategies that interact with different arms of
644 host immunity.

645 Previous studies have showed that entomopathogenic fungi have evolved
646 sophisticated strategies to evade phagocytosis by hemocytes. Once fungal spores
647 (conidia) germinate, penetrate host tegument and reach the hemocoel, fungi exist
648 within the hemocoel in the forms of blastospores with thinner cell walls than conidia
649 (*M. anisopliae*, *M. rileyi*, *B. bassiana*), and cell wall-free protoplasts (*E. muscae*).
650 (Wang and St. Leger, 2006) had demonstrated that host hemocytes can ingest conidia
651 of *M. anisopliae*, but are unable to recognize blastospore, due to the production of a
652 cell surface hydrophobic protein gene *Mcl1* that is expressed within 20 min of the
653 fungal pathogen contacting hemolymph. Studies have shown that blastospores of *B.*
654 *bassiana* and *M. anisopliae* can be phagocytosed at the early stages of infection but
655 manage to escape from host cells and continue to propagate. Growing hyphal bodies
656 can deform the plasmatocyte cell membrane, and the hemocyte count gradually
657 decreases as observed in Lepidopteran insect during fungal infection (Gillespie et al.,
658 2000; Hung and Boucias, 1992; Li et al., 2020a; Liu et al., 2019; Vilcinskas et al.,
659 1997). There are also evidences that the fungal toxins destruxins (DTXs) alter
660 circulating hemocytes of *G. mellonella* larvae (Vey et al., 2002; Vilcinskas et al.,
661 1997). But in *Drosophila*, Destruxin does not appear to affect *Drosophila* cellular
662 immune responses *in vivo* but would rather suppress the humoral immune response in

663 *Drosophila* (Pal et al., 2007). Here, the use of *NimC1*^{1}*; Eater*^{1} did not reveal any
664 major role of plasmatocytes in host defense against the five entomopathogenic fungi.
665 Flies lacking these two receptors are unable to phagocyte bacteria, latex beads or
666 apoptotic corpses (Bretscher et al., 2015; Dolgikh et al., 2025; Melcarne et al., 2019b)
667 and have lost the ability to bind to *M. anisopliae* spores (Figs. S1E, F). The
668 observation that hemoless flies lacking hemocytes due to the over-expression of *Bax*
669 display a wild-type survival rate to *B. bassiana* also support the notion that the
670 humoral response is more critical than cellular response to combat this
671 entomopathogenic fungus (Figs. S1A, B). We did however observe an increased
672 susceptibility of hemoless flies to *M. anisopliae* (Figs. S1C, D) pointing to a role of
673 hemocytes against this species that could not be uncovered with *NimC1*^{1}*; eater*^{1} fly
674 line. While the cellular response is important against yeast like *C. glabrata* (Quintin et
675 al., 2013), filamentous fungi may evade phagocytosis by reducing the exposition of
676 surface molecule(s) that are associated with non-self-recognition, as inferred in
677 studies in other insects (Gillespie et al., 2000; Wang and St. Leger, 2006). Additional
678 studies are required to better define the role of the cellular response to
679 entomopathogenic fungi.

680 A key aim of our study was to compare *Drosophila* immune responses to fungi
681 with distinct ecological strategies. Despite lifestyle differences, we found a largely
682 conserved requirement for Toll signaling, antifungal peptides, and melanization
683 across all species tested. However, notable differences emerged. The two generalist
684 entomopathogenic species strongly activate the Toll pathway but can overcome Toll
685 effectors to infect and kill flies. Studies have shown that these species express many
686 virulence factors that likely confers them protection against the host immune system
687 (Gao et al., 2011; Hu et al., 2014; Wang and Wang, 2017; Yuan et al., 2020). In
688 contrast, *A. fumigatus* is weakly pathogenic upon natural infection and accordingly
689 does not activate the Toll pathway. This opportunistic fungus does not have the ability
690 to effectively cross the cuticle of *Drosophila*, reflecting an opportunistic lifestyle. In
691 contrast the specialist noctuid-virulent fungus *M. rileyi* was moderately pathogenic to
692 flies and only triggered the Toll pathway at a late time point. This may reflect the
693 proliferation of this species within the host under a yeast-like blastospore form with a

694 thinner cell wall (Boucias et al., 2016; Liu et al., 2019), that would be less recognized
695 by the sensors acting upstream of the Toll pathway. This infectious strategy differs
696 from the toxin-mediated pathogenesis seen in *B. bassiana* and *M. anisopliae* during
697 fly colonization (Boucias et al., 2016; Schrank and Vainstein, 2010; Wang and Wang,
698 2017; Wang et al., 2021). Strikingly, we observed that *E. muscae* was greatly
699 pathogenic to flies but did not trigger a strong Toll pathway response. Nevertheless,
700 the Toll and melanization modules do contribute to host defense to *E. muscae*
701 indicating that this species is also sensitive to immune effectors. Our study finds that
702 *E. muscae* has developed a specific colonization strategy to escape the host immune
703 response. After crossing the cuticle barrier and reaching the hemolymph, *E. muscae*
704 grows as multinucleated protoplasts undetected by the immune system. The absence
705 of cell wall in protoplasts results in little glucan release into the hemolymph, which
706 might prevent recognition. This strategy would explain the high pathogenicity of *E.*
707 *muscae,* allowing growth hidden from the immune system, and only differentiating
708 into thinner cell-walled hyphae only shortly before the death of the host. While we
709 cannot however rule out that the high pathogenicity of *E. muscae* may also be partly
710 due to the fungus's increased resilience to immune effectors, we favor the
711 interpretation that it is instead mainly driven by its capacity to evade immune
712 detection. Similar escape strategies to hide from the host immune response have been
713 described in specialists such as *M. rileyi* and *O. sinensis* (Boucias et al., 2016; Li et al.,
714 2020b; Liu et al., 2019). Thus, two distinct infection strategies emerge among
715 entomopathogenic fungi: (1) Generalists, such as *B. bassiana* and *M. anisopliae*,
716 mount an aggressive infection, are immediately recognized by the immune system,
717 and rely on a broad array of virulence factors to counter host defenses (Gao et al.,
718 2011; Schrank and Vainstein, 2010; Wang et al., 2021); and (2) Specialists, such as *E.*
719 *muscae*, *M. rileyi*, and *O. sinensis*, adopt stealthier strategies, growing initially in
720 immune-evasive forms before lately transitioning to lethal hyphal stages. These
721 strategies appear to correlate with the fast and slow timing of host infection: for
722 example, *O. sinensis* persists for months in *Thitarodes* larvae, only initiating
723 pathogenic development later (Liu et al., 2019; Meng et al., 2015; Rao et al., 2019).
724 Similarly, the slow-growing, behavior-manipulating *E. muscae* may rely on immune

725 evasion to enable host manipulation and spore dispersal.

726 Taken together, our study clarifies the immune strategies employed by *D.*
727 *melanogaster* to combat fungal infections. We further provide insight on how
728 entomopathogenic fungi circumvent the immune response. Our study complements
729 the recent identification of fungal virulence factors required to disarm the immune
730 system (Lu et al., 2024; Shang et al., 2023; Tang et al., 2025). The interplay between
731 local and systemic immune responses highlights the complexity of antifungal defense
732 mechanisms in *Drosophila*. Understanding the evolutionary pressures that shape
733 immune responses to fungal pathogens could have broader implications for
734 controlling fungal infections in both natural and agricultural settings.

735

736 **Materials and methods**

737 **Fly stocks**

738 The fly stocks iso w^{1118} drosdel wild-type was used as the genetic background for
739 mutant isogenization (Ferreira et al., 2014). For survival experiments, w^{1118} *drosdel*,
740 Oregon R or Canton S flies were used as wild-type controls. To determine the
741 contribution of the four main immune modules to survive different fungal species, the
742 *Relish* (Rel^{E20}), *spätzle* (spz^{rm7}), *PPO1* and *PPO2* double mutant ($PPO1^{\Delta}$, $PPO2^{\Delta}$),
743 $NimC^{1}$ and *eater* double mutant ($Nim\ C1^{1}$; $Eater^{1}$) (Binggeli et al., 2014; Dudzic et al.,
744 2019; Hedengren et al., 1999; Lemaitre et al., 1996; Melcarne et al., 2019a) were used.
745 The fly line devoid of all four immune modules: Imd, Toll, Phagocytosis and
746 Melanization [genotype: *Def(Hayan-psh)*; *NimC1; Eater*, $Relish^{E20}$] (Ryckebusch et
747 al., 2025) is used to investigate whether immune modules function independently or
748 synergistically to combat different fungi.

749 To compare the importance of Toll sensing pathway, we used flies lacking Hayan
750 ($Hayan^{SK6}$), Psh (psh^{SK1}), both Hayan and Psh ($Hayan\text{-}psh^{def}$) (Dudzic et al., 2019),
751 Gram-negative bacteria binding protein 3 ($GNBP3^{hades}$) (Gottar et al., 2006), ModSP
752 ($modSP^{1}$), both Psh and ModSP (psh^{1};;$modSP^{1}$) (Buchon et al., 2009).

753 To determine the role of host defense peptides to combat fungal infection, we used
754 flies deleting ten of the twelve Bomanins ($Bom^{\Delta 55C}$) (Clemmons et al., 2015) and flies
755 lacking Metchnikowin (Mtk^{R1}), Drosomycin (Drs^{R1}) (Hanson et al., 2019), Baramicin

(*BaraA*$^{\Delta}$) (Hanson et al., 2021), Daisho 1, 2 ($^{\Delta}$*Dso*) (Cohen et al., 2020), as well as compound mutants *Mtk*^{R1};*Drs*^{R1}, *ΔAMP10* and *ΔAMP14* (Carboni et al., 2022; Hanson et al., 2019). In this study, we generated four new compounds mutants lack host defense peptides in the Drosdel background, (*BaraA*^{SW1}, *ΔDso*); (*Mtk*^{R}, *BaraA*^{SW11}; *Drs*^{R1}); (*Mtk*^{R}, *BaraA*^{SW1}, *ΔDso* ^{1}; *Drs*^{R1}) and (*Mtk* ^{R1}, *Bom* $^{\Delta 55C}$; *Drs*^{R1}). The *Hml* $^{\Delta}$ *-GAL4, UAS-GFP* fly line and UAS-Bax were used to delete hemocytes as described in (Defaye et al., 2009; Gaumer et al., 2000). We used a newly generated *w;; Hml*^{P2A}*-GAL4, UAS-CaMPARI2* to monitor hemocyte number and localization upon fungal infection (Moeyaert et al., 2018; Stephenson et al., 2022) The wild-type and mutant flies used in this study are listed in Table S1.

Microbial cultures

The wild type strains of *B. bassiana* 802, *M. anisopliae* ARSEF 2575, *M. rileyi* PHP1705 and the genetic strains *M. anisopliae* tagged GFP were cultured on malt agar (1g Bacteriological Peptone, 20g Glucose, 20 g Malt Extract, 15 g Agar, with the addition of water to the total volume of 1 liter) at 29°C for two weeks for harvesting conidial spores. The wild type strain *A. fumigatus* was cultured on malt agar at 37°C for one week for harvesting spores. Fungal materials were then strained through three layers of precision wipes with sterile water to collect spores, which were resuspended with 0.05% Tween 80 before being used for infection. The *E. muscae* ARSEF 454 was cultured in Grace's Insect Medium supplemented with 10% fetal bovine serum at 21°C. A liquid of 1 ml growing cultures after three weeks culture was transferred to a new cell culture flask with the addition of 10 ml media to maintain the fungal strains *in vitro*. The Gram-positive bacteria *Micrococcus luteus* were cultured on Luria Broth at 37°C and the optical density of the pellet (O.D.) at 600 nm 200 were used for infection.

Survival experiments

Survival experiments were conducted by both topical infection (natural infection) and systemic infection (septic infection), with twenty 2- to 4-day-old adult males per vial with two to three replicate experiments. Topical infection assays were performed

787 by immersing flies in spore suspensions for 30 s. The following concentrations (in
788 spores/ml) of spore suspensions were used: *A. fumigatus, B. bassiana* and *M. rileyi*: 1
789 × 10^9; *M. anisopliae*: 5 × 10^8. For *E. muscae* natural infection, about twenty-five 1- to
790 2-day-old adult male flies were infected by spore shower from twenty freshly
791 emerged cadavers that were previously injected with protoplasts for 24 h. The average
792 spores ejected from each female or male fly for 24 h were evaluated as described in
793 (Edwards and De Fine Licht, 2024). Briefly, the head of the cadaver was insert into
794 Vaseline inside the lid of the 2 ml tube containing 1ml 1% Triton-X and 0.2% maleic
795 acid solution for a period 24 h to collect ejected of spores. Then, spores in solution
796 were counted on a hemocytometer under a microscope. Systemic infections were
797 performed by pricking 2- to 4- day-old adult males in the thorax with a 100 µm-thick
798 insect pin dipped into spore suspensions. The following concentrations (in spores/ml)
799 of spore suspensions were used: *B. bassiana, M. anisopliae* and *M. rileyi*: 1× 10^8, *A.*
800 *fumigatus*: 1 × 10^9. Infected flies were flipped at the end of the first day and
801 maintained at 29℃ and flipped every two days later. Systemic infection with *E.*
802 *muscae* was performed by injecting 23 nl of protoplast suspension per fly with a
803 concentration of 2× 10^6 protoplasts/ml in PBS. The mortality was recorded daily. At
804 least three independent experiments for survival to infection were performed with 20
805 flies per vial on standard fly medium.
806
807 **Gene expression levels by RT-qPCR**
808 To investigate the immune responses to fungal infections, we performed the
809 quantitative reverse transcription PCR (qRT-PCR) analysis of Drs and BomBc3 used
810 as read-outs of Toll pathway activity. About 10 adult flies were collected at indicated
811 time points and homogenized for RNA extraction using TRIzol reagent. The total
812 RNA was resuspended in RNase-free water and 0.5 mg of total RNA in 10 ml
813 reactions was reverse transcribed using PrimeScript RT (TAKARA) with random
814 hexamer and oligo dT primers. Quantitative PCR was performed on a LightCycler
815 480 (Roche) in 96-well plates using PowerUp SYBR Green Master Mix. Primers
816 were listed in Table S2. The expression of *Drs* was also investigated by observing
817 GFP intensity of *Drs-GFP* flies after fungal infection (Ferrandon, 1998). Infected flies

818 were anesthetized with CO_2 and observed for fluorescence with a Leica Application
819 SuiteX and LEICA DFC 7000T camera.
820
821 **Quantitation of fungal loads for kinetic growth**
822 Fungal load in infected flies was measured either by qPCR or by fluorescence
823 intensity of *M. anisopliae t*agged GFP. Adult male flies infect with *B. bassiana* and *M.*
824 *anisopliae* were incubated at 29°C and *E. muscae* at 21°C. Groups of 10 flies were
825 sampled at indicated time points and frozen in liquid nitrogen. The total DNA of each
826 sample was extracted with DNeasy Plant Mini Kit (Qiagen). Fungal loads of *B.*
827 *bassiana* and *E. muscae* was quantified by fungal ribosomal protein 18S rRNA
828 relative to the *Drosophila* ribosomal protein Rpl32 (Rp49), while fungal load of *M.*
829 *anisopliae* was quantified by fungal ribosomal protein Rpl32 relative to *Drosophila*
830 protein Actin. Primers were listed in Table S2.
831 *M. anisopliae* tagged GFP was also used to investigate the growth of fungi inside
832 the flies after pricking. The infected flies were anesthesized with CO_2 and observed
833 for fluorescence with a Leica Application SuiteX and LEICA DFC 7000T camera.
834
835 **Ex-vivo phagocytosis assay with microscopy**
836 Five third-instar larvae were cleaned and dissected in 150 μL of Schneider's
837 medium, ensuring that vital organs remained intact. The samples were incubated with
838 approximately 10^5 bacterial bioparticles or fungal blastospores in a humidified
839 chamber for 2 hours. Cells were then fixed with 4% paraformaldehyde (PFA) and
840 stained with phalloidin (1:200) for 1 hour at room temperature, followed by three
841 washes with 1× PBS. Finally, slides were mounted with a mounting medium and
842 sealed with nail polish. Hemocytes were imaged using an inverted Evident confocal
843 microscope equipped with a 60× oil immersion lens. Maximum Z-projections were
844 generated for analysis using FIJI/ImageJ software.
845
846 **Ex-vivo phagocytosis assay with FACS**
847 Five third-instar larvae were surface-sterilized and bled into 130 μL of Schneider's
848 medium within 2 minutes. The hemolymph was collected in Protein Lo-Bind

849 Eppendorf tubes to minimize sample loss. Approximately 10^5 bacterial bioparticles or
850 fungal blastospores were added to the hemocyte suspension and incubated at room
851 temperature for 2 hours. Following incubation, the samples were placed on ice, and
852 hemocytes were immediately analyzed using a CytoFLEX flow cytometer (Beckman
853 Coulter) to measure the fraction of cells phagocytosing. 60 µl volume was read at
854 medium speed (40 µl/min).

855 Hemocytes from Hml GAL4, UAS-GFP larvae were used to define the hemocyte
856 population for flow cytometry analysis. GFP-positive cells were identified and gated
857 based on fluorescence detected in the B525 channel, enabling the exclusion of debris
858 and non-hemocytic events. The same gating strategy was applied consistently across
859 all genotypes to track the hemocyte population and to quantify the proportion of
860 hemocytes exhibiting fluorescence corresponding to internalized bacterial bioparticles
861 or fungal spores. The percentage of hemocytes phagocytosing (*f*) was calculated using
862 the following equations:

$$f = \frac{\text{Number of hemocytes in fluorescence positive gate}}{\text{Total number of hemocytes}}$$

863

864

865 **Statistical analysis**

866 Statistical analyses were performed using GraphPad Prism 10 software. Survival
867 experiments were repeated at least three times independently with 20 flies per
868 treatment. Statistical significance of survival data was calculated with a log-rank test
869 (Mantel-Cox test) comparing each genotype to w^{1118} flies. Quantitative PCR data and
870 fungal load data were compared by One-way ANOVA following Tukey's multiple
871 comparisons test. The full statistic models and outputs of Figures are listed in Table
872 S3. P values of < 0.05 = *, < 0.01 = **, < 0.001 = ***, and < 0.0001 = **** were
873 considered significant. ns indicates non-significant, P>0.05. Error bars represent the
874 standard deviation (s.d.) of replicate experiments.

875

876 **Acknowledgments**

877 We thank Samuel Rommelaere, Jean-Philippe Boquette, Fanny Schüpfer for
878 experimental help. We thank Kathryn Bushley and Carolyn Elya for providing the

Entomophthora muscae strains used for this study. Guiqing Liu stay in the Lemaitre lab was supported by funding from the China Scholarship Council (CSC, No. 202208440111) and the SNSF grant TMAG-3_225935. We thank Vienna Drosophila Resource Center (VDRC) and the Bloomington stock center for fly stocks. This project was supported by the SNSF grants (310030_215073).

Author Contributions

Conceived and designed the experiments: GQL BL. Performed the experiments: GQL YT JL PKS. Analyzed the data: GQL YT PKS BL. Contributed reagents/ materials/analysis tools: MAH BL. Wrote the paper: GQL MAH BL.

References

Almaliki HS, Niu M, Keller NP, Yin G, Bennett JW. 2023. Mutational analysis of aspergillus fumigatus volatile oxylipins in a Drosophila eclosion assay. Journal of Fungi **9**:402. DOI: https://doi.org/10.3390/jof9040402

Ballou ER, Avelar GM, Childers DS, Mackie J, Bain JM, Wagener J, Kastora SL, Panea MD, Hardison SE, Walker LA, Erwig LP, Munro CA, Gow NAR, Brown GD, MacCallum DM, Brown AJP. 2016. Lactate signalling regulates fungal β-glucan masking and immune evasion. Nature Microbiology **2**:16238. DOI: https://doi.org/10.1038/nmicrobiol.2016.238

Binggeli O, Neyen C, Poidevin M, Lemaitre B. 2014. Prophenoloxidase activation is required for survival to microbial infections in Drosophila. PLoS Pathogens **10**:e1004067. DOI: https://doi.org/10.1371/journal.ppat.1004067

Boucias D, Liu S, Meagher R, Baniszewski J. 2016. Fungal dimorphism in the entomopathogenic fungus Metarhizium rileyi: Detection of an in vivo quorum-sensing system. Journal of Invertebrate Pathology **136**:100–108. DOI: https://doi.org/10.1016/j.jip.2016.03.013

Bretscher AJ, Honti V, Binggeli O, Burri O, Poidevin M, Kurucz E, Zsamboki J, Ando I, Lemaitre B. 2015. The Nimrod transmembrane receptor Eater is required for hemocyte attachment to the sessile compartment in Drosophila melanogaster. Biol Open **4**:355–63. DOI: https://doi.org/10.1242/bio.201410595

Brown AJP. 2023. Fungal resilience and host–pathogen interactions: Future perspectives and opportunities. Parasite Immunology **45**:e12946. DOI: https://doi.org/10.1111/pim.12946

Buchon N, Poidevin M, Kwon H-M, Guillou A, Sottas V, Lee B-L, Lemaitre B. 2009. A single modular serine protease integrates signals from pattern-recognition receptors upstream of the Drosophila Toll pathway. Proceedings of the National Academy of Sciences **106**:12442–12447. DOI: https://doi.org/10.1073/pnas.0901924106

Capilla A, Karachentsev D, Patterson RA, Hermann A, Juarez MT, McGinnis W. 2017. Toll pathway is required for wound-induced expression of barrier repair genes in the Drosophila epidermis. Proceedings of the National Academy of Sciences **114**. DOI: https://doi.org/10.1073/pnas.1613917114

Carboni AL, Hanson MA, Lindsay SA, Wasserman SA, Lemaitre B. 2022. Cecropins contribute to Drosophila host defense against a subset of fungal and Gram-negative bacterial infection. Genetics **220**:iyab188. DOI: https://doi.org/10.1093/genetics/iyab188

Carvalho L, Jacinto A, Matova N. 2014. The Toll/NF-κB signaling pathway is required for epidermal wound repair in Drosophila. Proceedings of the National Academy of Sciences **111**. DOI: https://doi.org/10.1073/pnas.1408224111

Casalini G, Giacomelli A, Antinori S. 2024. The WHO fungal priority pathogens list: a crucial reappraisal to review the prioritisation. The Lancet Microbe **5**:717–724. DOI: https://doi.org/10.1016/S2666-5247(24)00042-9

Cen K, Li B, Lu Y, Zhang S, Wang C. 2017. Divergent LysM effectors contribute to the virulence of Beauveria bassiana by evasion of insect immune defenses. PLOS Pathogens **13**:e1006604. DOI: https://doi.org/10.1371/journal.ppat.1006604

Clemmons AW, Lindsay SA, Wasserman SA. 2015. An effector peptide family required for Drosophila Toll-mediated immunity. PLOS Pathogens **11**:e1004876. DOI: https://doi.org/10.1371/journal.ppat.1004876

Cohen LB, Lindsay SA, Xu Y, Lin SJH, Wasserman SA. 2020. The Daisho peptides mediate Drosophila defense against a subset of filamentous fungi. Frontiers in Immunology **11**:9. DOI: https://doi.org/10.3389/fimmu.2020.00009

De Fine Licht HH, Jensen AB, Eilenberg J. 2017. Comparative transcriptomics reveal host-specific nucleotide variation in entomophthoralean fungi. Molecular Ecology **26**:2092–2110. DOI: https://doi.org/10.1111/mec.13863

De Gregorio E. 2002. The Toll and Imd pathways are the major regulators of the immune response in Drosophila. The EMBO Journal **21**:2568–2579. DOI: https://doi.org/10.1093/emboj/21.11.2568

Dean R, Van Kan JAL, Pretorius ZA, Hammond-Kosack KE, Di Pietro A, Spanu PD, Rudd JJ, Dickman M, Kahmann R, Ellis J, Foster GD. 2012. The Top 10 fungal pathogens in molecular plant pathology. Molecular Plant Pathology **13**:414–430. DOI: https://doi.org/10.1111/j.1364-3703.2011.00783.x

Defaye A, Evans I, Crozatier M, Wood W, Lemaitre B, Leulier F. 2009. Genetic Ablation of Drosophila Phagocytes Reveals Their Contribution to Both Development and Resistance to Bacterial Infection. Journal of Innate Immunity **1**:322–334. DOI: https://doi.org/10.1159/000210264

Dolgikh A, Rommelaere S, Ghanem A, Petrignani B, Poidevin M, Kurant E, Lemaitre B. 2025. The secreted Nimrod protein NimB1 negatively regulates early steps of apoptotic cell phagocytosis in Drosophila. Development **152**:dev204919. DOI: https://doi.org/10.1242/dev.204919

Dudzic JP, Hanson MA, Iatsenko I, Kondo S, Lemaitre B. 2019. More than black or white: Melanization and Toll share regulatory serine proteases in Drosophila. Cell Reports **27**:1050-1061.e3. DOI: https://doi.org/10.1016/j.celrep.2019.03.101

Edwards S, De Fine Licht HH. 2024. Rearing zombie flies: Laboratory culturing of the behaviourally manipulating fungal pathogen Entomophthora muscae. MethodsX **12**:102523. DOI: https://doi.org/10.1016/j.mex.2023.102523

Ekengren S. 1999. Drosophila cecropin as an antifungal agent. Insect Biochemistry and Molecular Biology **29**:965–972. DOI: https://doi.org/10.1016/S0965-1748(99)00071-5

Ekengren S, Hultmark D. 1999. Drosophila cecropin as an antifungal agent. Insect Biochemistry and Molecular Biology **29**:965–972. DOI: https://doi.org/10.1016/S0965-1748(99)00071-5

El Chamy L, Leclerc V, Caldelari I, Reichhart J-M. 2008. Sensing of “danger signals” and pathogen-associated molecular patterns defines binary signaling pathways “upstream” of Toll. Nature Immunology **9**:1165–1170. DOI: https://doi.org/10.1038/ni.1643

Elya C, De Fine Licht HH. 2021. The genus Entomophthora: bringing the insect destroyers into the twenty-first century. IMA Fungus **12**:34. DOI: https://doi.org/10.1186/s43008-021-00084-w

Elya C, Lok TC, Spencer QE, McCausland H, Martinez CC, Eisen M. 2018. Robust manipulation of the behavior of Drosophila melanogaster by a fungal pathogen in the laboratory. eLife **7**:e34414. DOI: https://doi.org/10.7554/eLife.34414

Fehlbaum P, Bulet P, Michaut L, Lagueux M, Broekaert WF, Hetru C, Hoffmann JA. 1994. Insect immunity. Septic injury of Drosophila induces the synthesis of a potent antifungal peptide with sequence homology to plant antifungal peptides. Journal of Biological Chemistry **269**:33159–33163. DOI: https://doi.org/10.1016/S0021-9258(20)30111-3

Feldman MB, Vyas JM, Mansour MK. 2019. It takes a village: Phagocytes play a central role in fungal immunity. Seminars in Cell & Developmental Biology **89**:16–23. DOI: https://doi.org/10.1016/j.semcdb.2018.04.008

Ferrandon D. 1998. A drosomycin-GFP reporter transgene reveals a local immune response in Drosophila that is not dependent on the Toll pathway. The EMBO Journal **17**:1217–1227. DOI: https://doi.org/10.1093/emboj/17.5.1217

Ferreira ÁG, Naylor H, Esteves SS, Pais IS, Martins NE, Teixeira L. 2014. The Toll-Dorsal pathway is required for resistance to viral oral infection in Drosophila. PLoS Pathogens **10**:e1004507. DOI: https://doi.org/10.1371/journal.ppat.1004507

Gao Q, Jin K, Ying S-H, Zhang Y, Xiao G, Shang Y, Duan Z, Hu X, Xie X-Q, Zhou G, Peng G, Luo Z, Huang W, Wang B, Fang W, Wang S, Zhong Y, Ma L-J, St. Leger RJ, Zhao G-P, Pei Y, Feng M-G, Xia Y, Wang C. 2011. Genome sequencing and comparative transcriptomics of the model entomopathogenic fungi Metarhizium anisopliae and M. acridum. PLoS Genetics **7**:e1001264. DOI: https://doi.org/10.1371/journal.pgen.1001264

Gaumer S, Guenal I, Brun S, Theodore L, Mignotte B. 2000. Bcl-2 and Bax mammalian regulators of apoptosis are functional in Drosophila. Cell Death Differ **7**:804–14. DOI: https://doi.org/10.1038/sj.cdd.4400714

Gillespie JP, Bailey AM, Cobb B, Vilcinskas A. 2000. Fungi as elicitors of insect immune responses. Archives of Insect Biochemistry and Physiology **44**:49–68. DOI: https://doi.org/10.1002/1520-6327(200006)44:2%253C49::AID-ARCH1%253E3.0.CO;2-F

Gladieux P, Ropars J, Badouin H, Branca A, Aguileta G, De Vienne DM, Rodríguez De La Vega RC, Branco S, Giraud T. 2014. Fungal evolutionary genomics provides insight into the mechanisms of adaptive divergence in eukaryotes. Molecular Ecology **23**:753–773. DOI: https://doi.org/10.1111/mec.12631

Gottar M, Gobert V, Matskevich AA, Reichhart J-M, Wang C, Butt TM, Belvin M, Hoffmann JA. 2006. Dual detection of fungal infections in Drosophila through recognition of microbial structures and sensing of virulence factors. **127**:1425–1437.

Hanson M, Westlake H, Bulet P, Lemaitre B. 2025. The antimicrobial and host defense peptides of Drosophila Melanogaster. Annual Review of Microbiology.

Hanson MA. 2024. When the microbiome shapes the host: immune evolution implications for infectious disease. Philosophical Transactions of the Royal Society B: Biological Sciences **379**:20230061. DOI: https://doi.org/10.1098/rstb.2023.0061

Hanson MA, Cohen LB, Marra A, Iatsenko I, Wasserman SA, Lemaitre B. 2021. The Drosophila Baramicin polypeptide gene protects against fungal infection. PLOS Pathogens **17**:e1009846. DOI: https://doi.org/10.1371/journal.ppat.1009846

Hanson MA, Dostálová A, Ceroni C, Poidevin M, Kondo S, Lemaitre B. 2019. Synergy and remarkable specificity of antimicrobial peptides in vivo using a systematic knockout approach. eLife **8**:e44341. DOI: https://doi.org/10.7554/eLife.44341

Hanson MA, Grollmus L, Lemaitre B. 2023. Ecology-relevant bacteria drive the evolution of host antimicrobial peptides in Drosophila. Science **381**:eadg5725. DOI: https://doi.org/10.1126/science.adg5725

Hedengren M, BengtÅsling, Dushay MS, Ando I, Ekengren S, Wihlborg M, Hultmark D. 1999. Relish, a central factor in the control of humoral but not cellular immunity in Drosophila. Molecular Cell **4**:827–837. DOI: https://doi.org/10.1016/s1097-2765(00)80392-5

Hong S, Sun Y, Sun D, Wang C. 2022. Microbiome assembly on Drosophila body surfaces benefits the flies to combat fungal infections. iScience **25**:104408. DOI: https://doi.org/10.1016/j.isci.2022.104408

Hu X, Xiao G, Zheng P, Shang Y, Su Y, Zhang X, Liu X, Zhan S, St. Leger RJ, Wang C. 2014. Trajectory and genomic determinants of fungal-pathogen speciation and host adaptation. Proceedings of the National Academy of Sciences **111**:16796–16801. DOI: https://doi.org/10.1073/pnas.1412662111

Huang J, Lou Y, Liu J, Bulet P, Cai C, Ma K, Jiao R, Hoffmann JA, Liégeois S, Li Z, Ferrandon D. 2023. A Toll pathway effector protects Drosophila specifically from distinct toxins secreted by a fungus or a bacterium. Proceedings of the National Academy of Sciences **120**:e2205140120. DOI: https://doi.org/10.1073/pnas.2205140120

Hughes DP, Andersen SB, Hywel-Jones NL, Himaman W, Billen J, Boomsma JJ. 2011. Behavioral mechanisms and morphological symptoms of zombie ants dying from fungal infection. BMC Ecology **11**:13. DOI: https://doi.org/10.1186/1472-6785-11-13

Hung SY, Boucias D. 1992. Influence of Beauveria bassiana on the cellular defense response of the beet armyworm, Spodoptera exigua. Journal of Invertebrate Pathology **60**:152–158. DOI: https://doi.org/10.1016/0022-2011(92)90089-M

Issa N, Guillaumot N, Lauret E, Matt N, Schaeffer-Reiss C, Van Dorsselaer A, Reichhart J-M, Veillard F. 2018. The circulating protease persephone is an immune sensor for microbial proteolytic activities upstream of the Drosophila Toll pathway. Molecular Cell **69**:539-550.e6. DOI: https://doi.org/10.1016/j.molcel.2018.01.029

Jang I-H, Chosa N, Kim S-H, Nam H-J, Lemaitre B, Ochiai M, Kambris Z, Brun S, Hashimoto C, Ashida M, Brey PT, Lee W-J. 2006. A spätzle-processing enzyme required for toll signaling activation in drosophila innate immunity. Developmental Cell **10**:45–55. DOI: https://doi.org/10.1016/j.devcel.2005.11.013

Kambris Z, Brun S, Jang I-H, Nam H-J, Romeo Y, Takahashi K, Lee W-J, Ueda R, Lemaitre B. 2006. Drosophila immunity: A large-scale in vivo RNAi screen identifies five serine proteases required for toll activation. Current Biology **16**:808–813. DOI: https://doi.org/10.1016/j.cub.2006.03.020

Lai Y, Jiang B, Hou F, Huang X, Ling B, Lu H, Zhong T, Huang J. 2023. The emerging role of extracellular vesicles in fungi: a double-edged sword. Frontiers in Microbiology **14**:1216895. DOI: https://doi.org/10.3389/fmicb.2023.1216895

Lazzaro BP, Zasloff M, Rolff J. 2020. Antimicrobial peptides: Application informed by evolution.

Science **368**:eaau5480. DOI: https://doi.org/10.1126/science.aau5480

Lemaitre B, Nicolas E, Michaut L, Reichhart J-M, Hoffmann JA. 1996. The dorsoventral regulatory gene cassette spätzle/toll/cactus controls the potent antifungal response in Drosophila adults. Cell **86**:973–983. DOI: https://doi.org/10.1016/S0092-8674(00)80172-5

Levashina EA, Ohresser S, Bulet P, Reichhart J, Hetru C, Hoffmann JA. 1995. Metchnikowin, a Novel Immune-Inducible Proline-Rich Peptide from Drosophila with Antibacterial and Antifungal Properties. European Journal of Biochemistry **233**:694–700. DOI: https://doi.org/10.1111/j.1432-1033.1995.694_2.x

Levitin A, Whiteway M. 2008. Drosophila innate immunity and response to fungal infections. Cellular Microbiology **10**:1021–1026. DOI: https://doi.org/10.1111/j.1462-5822.2008.01120.x

Li M, Meng Q, Zhang H, Ni R, Zhou G, Zhao Y, Wu P, Shu R, Qin Q, Zhang J. 2020a. Vegetative development and host immune interaction of Ophiocordyceps sinensis within the hemocoel of the ghost moth larva, Thitarodes xiaojinensis. Journal of Invertebrate Pathology **170**:107331. DOI: https://doi.org/10.1016/j.jip.2020.107331

Li M, Meng Q, Zhang H, Ni R, Zhou G, Zhao Y, Wu P, Shu R, Qin Q, Zhang J. 2020b. Vegetative development and host immune interaction of Ophiocordyceps sinensis within the hemocoel of the ghost moth larva, Thitarodes xiaojinensis. Journal of Invertebrate Pathology **170**:107331. DOI: https://doi.org/10.1016/j.jip.2020.107331

Liu G, Han R, Cao L. 2019. Artificial cultivation of the chinese cordyceps from injected ghost moth larvae. Environmental Entomology **48**:1088–1094. DOI: https://doi.org/10.1093/ee/nvz099

Lohse MB, Johnson AD. 2008. Differential Phagocytosis of White versus Opaque Candida albicans by Drosophila and Mouse Phagocytes. PLoS ONE **3**:e1473. DOI: https://doi.org/10.1371/journal.pone.0001473

Lou Y, Zhang B, Zhang Z, Pan Y, Yang J, Li L, Huang J, Yuan Z, Liegeois S, Bulet P, Xu R, Zi L, Ferrandon D. 2025. Distinct Bomanins at the Drosophila 55C locus function in resistance and resilience to infections. Annual Review of Entomology.

Lu M, Wei D, Shang J, Li S, Song S, Luo Y, Tang G, Wang C. 2024. Suppression of Drosophila antifungal immunity by a parasite effector via blocking GNBP3 and GNBP-like 3, the dual receptors for β-glucans. Cell Reports **43**:113642. DOI: https://doi.org/10.1016/j.celrep.2023.113642

Ma M, Luo J, Li C, Eleftherianos I, Zhang W, Xu L. 2024. A life-and-death struggle: interaction of insects with entomopathogenic fungi across various infection stages. Frontiers in Immunology **14**:1329843. DOI: https://doi.org/10.3389/fimmu.2023.1329843

Melcarne C, Lemaitre B, Kurant E. 2019a. Phagocytosis in Drosophila: From molecules and cellular machinery to physiology. Insect Biochemistry and Molecular Biology **109**:1–12. DOI: https://doi.org/10.1016/j.ibmb.2019.04.002

Melcarne C, Ramond E, Dudzic J, Bretscher AJ, Kurucz É, Andó I, Lemaitre B. 2019b. Two Nimrod receptors, NimC1 and Eater, synergistically contribute to bacterial phagocytosis in *Drosophila melanogaster*. The FEBS Journal. DOI: https://doi.org/10.1111/febs.14857

Meng Q, Yu H-Y, Zhang H, Zhu W, Wang M-L, Zhang J-H, Zhou G-L, Li X, Qin Q-L, Hu S-N, Zou Z. 2015. Transcriptomic insight into the immune defenses in the ghost moth, Hepialus xiaojinensis, during an Ophiocordyceps sinensis fungal infection. Insect Biochemistry and Molecular Biology **64**:1–15. DOI: https://doi.org/10.1016/j.ibmb.2015.06.014

Michel T, Reichhart J-M, Hoffmann JA, Royet J. 2001. Drosophila Toll is activated by Gram-positive

1094 bacteria through a circulating peptidoglycan recognition protein. Nature **414**:756–759. DOI:
1095 https://doi.org/10.1038/414756a
1096 Moeyaert B, Holt G, Madangopal R, Perez-Alvarez A, Fearey BC, Trojanowski NF, Ledderose J,
1097 Zolnik TA, Das A, Patel D, Brown TA, Sachdev RNS, Eickholt BJ, Larkum ME, Turrigiano GG, Dana H,
1098 Gee CE, Oertner TG, Hope BT, Schreiter ER. 2018. Improved methods for marking active neuron
1099 populations. Nature Communications **9**:4440. DOI: https://doi.org/10.1038/s41467-018-06935-2
1100 Moghaddam M-RB, Gross T, Becker A, Vilcinskas A, Rahnamaeian M. 2017. The selective
1101 antifungal activity of Drosophila melanogaster metchnikowin reflects the species-dependent
1102 inhibition of succinate–coenzyme Q reductase. Scientific Reports **7**:8192. DOI:
1103 https://doi.org/10.1038/s41598-017-08407-x
1104 Morelli KA, Kerkaert JD, Cramer RA. 2021. Aspergillus fumigatus biofilms: Toward understanding
1105 how growth as a multicellular network increases antifungal resistance and disease progression.
1106 PLOS Pathogens **17**:e1009794. DOI: https://doi.org/10.1371/journal.ppat.1009794
1107 Mpamhanga CD, Kounatidis I. 2024. The utility of Drosophila melanogaster as a fungal infection
1108 model. Frontiers in Immunology **15**. DOI: https://doi.org/10.3389/fimmu.2024.1349027
1109 Murante D, Hogan DA. 2024. Drivers of diversification in fungal pathogen populations. PLOS
1110 Pathogens **20**:e1012430. DOI: https://doi.org/10.1371/journal.ppat.1012430
1111 Nam H-J, Jang I-H, You H, Lee K-A, Lee W-J. 2012. Genetic evidence of a redox-dependent
1112 systemic wound response via Hayan Protease-Phenoloxidase system in Drosophila:
1113 Redox-modulated systemic wound response. The EMBO Journal **31**:1253–1265. DOI:
1114 https://doi.org/10.1038/emboj.2011.476
1115 Pal S, St. Leger RJ, Wu LP. 2007. Fungal Peptide Destruxin A Plays a Specific Role in Suppressing
1116 the Innate Immune Response in Drosophila melanogaster. Journal of Biological Chemistry
1117 **282**:8969–8977. DOI: https://doi.org/10.1074/jbc.M605927200
1118 Pradeu T, Thomma BPHJ, Girardin SE, Lemaitre B. 2024. The conceptual foundations of innate
1119 immunity: Taking stock 30 years later. Immunity **57**:613–631. DOI:
1120 https://doi.org/10.1016/j.immuni.2024.03.007
1121 Qu S, Wang S. 2018. Interaction of entomopathogenic fungi with the host immune system.
1122 Developmental & Comparative Immunology **83**:96–103. DOI:
1123 https://doi.org/10.1016/j.dci.2018.01.010
1124 Quintin J, Asmar J, Matskevich AA, Lafarge M-C, Ferrandon D. 2013. The Drosophila Toll pathway
1125 controls but does not clear Candida glabrata infections. The Journal of Immunology
1126 **190**:2818–2827. DOI: https://doi.org/10.4049/jimmunol.1201861
1127 Rao Z, Cao L, Wu H, Qiu X, Liu G, Han R. 2019. Comparative transcriptome analysis of thitarodes
1128 armoricanus in response to the entomopathogenic fungi paecilomyces hepiali and
1129 ophiocordyceps sinensis. Insects **11**:4. DOI: https://doi.org/10.3390/insects11010004
1130 Reis FCG, Rodrigues ML. 2025. Things you wanted to know about fungal extracellular vesicles (but
1131 were afraid to ask). PLOS Neglected Tropical Diseases **19**:e0013038. DOI:
1132 https://doi.org/10.1371/journal.pntd.0013038
1133 Ristow LC, Jezewski AJ, Chadwick BJ, Stamnes MA, Lin X, Krysan DJ. 2023. Cryptococcus
1134 neoformans adapts to the host environment through TOR-mediated remodeling of phospholipid
1135 asymmetry. Nature Communications **14**:6587. DOI: https://doi.org/10.1038/s41467-023-42318-y
1136 Rodrigues ML, May RC, Janbon G. 2024. The multiple frontiers in the study of extracellular
1137 vesicles produced by fungi. Microbes and Infection **26**:105233. DOI:

https://doi.org/10.1016/j.micinf.2023.105233
Rommelaere S, Carboni A, Bada Juarez JF, Boquete J-P, Abriata LA, Teixeira Pinto Meireles F, Rukes V, Vincent C, Kondo S, Dionne MS, Dal Peraro M, Cao C, Lemaitre B. 2024. A humoral stress response protects Drosophila tissues from antimicrobial peptides. Current Biology **34**:1426-1437.e6. DOI: https://doi.org/10.1016/j.cub.2024.02.049
Rommelaere S, Masson F, Lemaitre B. 2025. From foes to friends: Fundamental and applied insights on insect-microbe interactions in Overview of insect immunity and symbiosis: Interactions and implications. *Comprehensive Molecular Insect Science*. Elsevier.
Ryckebusch F, Tian Y, Rapin M, Schüpfer F, Hanson MA, Lemaitre B. 2025. Layers of immunity: Deconstructing the Drosophila effector response. bioRixv. DOI: https://doi.org/10.1101/2025.03.28.645959
Schrank A, Vainstein MH. 2010. Metarhizium anisopliae enzymes and toxins. Toxicon **56**:1267–1274. DOI: https://doi.org/10.1016/j.toxicon.2010.03.008
Shan T, Wang Y, Bhattarai K, Jiang H. 2023. An evolutionarily conserved serine protease network mediates melanization and Toll activation Drosophila. Science Advances **9**. DOI: https://doi.org/10.1126/sciadv.adk2756
Shang J, Tang G, Yang J, Lu M, Wang C-Z, Wang C. 2023. Sensing of a spore surface protein by a Drosophila chemosensory protein induces behavioral defense against fungal parasitic infections. Current Biology **33**:276-286.e5. DOI: https://doi.org/10.1016/j.cub.2022.11.004
Shang Y, Xiao G, Zheng P, Cen K, Zhan S, Wang C. 2016. Divergent and convergent evolution of fungal pathogenicity. Genome Biology and Evolution **8**:1374–1387. DOI: https://doi.org/10.1093/gbe/evw082
Siscar-Lewin S, Hube B, Brunke S. 2022. Emergence and evolution of virulence in human pathogenic fungi. Trends in Microbiology **30**:693–704. DOI: https://doi.org/10.1016/j.tim.2021.12.013
Soares MP, Teixeira L, Moita LF. 2017. Disease tolerance and immunity in host protection against infection. Nature Reviews Immunology **17**:83–96. DOI: https://doi.org/10.1038/nri.2016.136
Stephenson HN, Streeck R, Grüblinger F, Goosmann C, Herzig A. 2022. Hemocytes are essential for *Drosophila melanogaster* post-embryonic development, independent of control of the microbiota. Development **149**:dev200286. DOI: https://doi.org/10.1242/dev.200286
Tang G, Song S, Shang J, Luo Y, Li S, Wei D, Wang C. 2025. Fungal evasion of Drosophila immunity involves blocking the cathepsin-mediated cleavage maturation of the danger-sensing protease. Proceedings of the National Academy of Sciences **122**:e2419343122. DOI: https://doi.org/10.1073/pnas.2419343122
Unckless RL, Howick VM, Lazzaro BP. 2016. Convergent Balancing Selection on an Antimicrobial Peptide in Drosophila. Current Biology **26**:257–262. DOI: https://doi.org/10.1016/j.cub.2015.11.063
Uttenweiler-Joseph S, Moniatte M, Lagueux M, Van Dorsselaer A, Hoffmann JA, Bulet P. 1998. Differential display of peptides induced during the immune response of Drosophila: A matrix-assisted laser desorption ionization time-of-flight mass spectrometry study. Proceedings of the National Academy of Sciences **95**:11342–11347. DOI: https://doi.org/10.1073/pnas.95.19.11342
Valanne S, Wang J-H, Rämet M. 2011. The Drosophila Toll signaling pathway. The Journal of Immunology **186**:649–656. DOI: https://doi.org/10.4049/jimmunol.1002302

Valero-Jiménez CA, Wiegers H, Zwaan BJ, Koenraadt CJM, Van Kan JAL. 2016. Genes involved in virulence of the entomopathogenic fungus Beauveria bassiana. Journal of Invertebrate Pathology **133**:41–49. DOI: https://doi.org/10.1016/j.jip.2015.11.011

Vasanth S, Wang Y, Khan A, Xiong C, Boquete J-P, Shan T, Jiang H, Lemaitre B. 2025. The serine protease homolog Skanda modulates Toll-Phenoloxidase-mediated immunity in Drosophila. bioRxiv. DOI: https://doi.org/10.1101/2025.09.30.679548

Vertyporokh L, Hułas-Stasiak M, Wojda I. 2020. Host–pathogen interaction after infection of Galleria mellonella with the filamentous fungus Beauveria bassiana. Insect Science **27**:1079–1089. DOI: https://doi.org/10.1111/1744-7917.12706

Vey A, Matha V, Dumas C. 2002. Effects of the peptide mycotoxin destruxin E on insect haemocytes and on dynamics and efficiency of the multicellular immune reaction. Journal of Invertebrate Pathology **80**:177–187. DOI: https://doi.org/10.1016/S0022-2011(02)00104-0

Vilcinskas A, Matha V, Götz P. 1997. Inhibition of phagocytic activity of plasmatocytes isolated from Galleria mellonella by entomogenous fungi and their secondary metabolites. Journal of Insect Physiology **43**:475–483. DOI: https://doi.org/10.1016/S0022-1910(96)00120-5

Wang C, St. Leger RJ. 2006. A collagenous protective coat enables Metarhizium anisopliae to evade insect immune responses. Proceedings of the National Academy of Sciences **103**:6647–6652. DOI: https://doi.org/10.1073/pnas.0601951103

Wang C, Wang S. 2017. Insect pathogenic fungi: Genomics, molecular interactions, and genetic improvements. Annual Review of Entomology **62**:73–90. DOI: https://doi.org/10.1146/annurev-ento-031616-035509

Wang H, Lu Z, Keyhani NO, Deng J, Zhao X, Huang S, Luo Z, Jin K, Zhang Y. 2023. Insect fungal pathogens secrete a cell wall-associated glucanase that acts to help avoid recognition by the host immune system. PLOS Pathogens **19**:e1011578. DOI: https://doi.org/10.1371/journal.ppat.1011578

Wang H, Peng H, Li W, Cheng P, Gong M. 2021. The toxins of Beauveria bassiana and the strategies to improve their virulence to insects. Frontiers in Microbiology **12**:705343. DOI: https://doi.org/10.3389/fmicb.2021.705343

Weber ANR, Tauszig-Delamasure S, Hoffmann JA, Lelièvre E, Gascan H, Ray KP, Morse MA, Imler J-L, Gay NJ. 2003. Binding of the Drosophila cytokine Spätzle to Toll is direct and establishes signaling. Nature Immunology **4**:794–800. DOI: https://doi.org/10.1038/ni955

Westlake H, Hanson MA, Lemaitre B. 2024. The Drosophila immunity handbook, First. EPFL Press. DOI: https://doi.org/10.55430/6304tdihva01

Wichadakul D, Kobmoo N, Ingsriswang S, Tangphatsornruang S, Chantasingh D, Luangsa-ard JJ, Eurwilaichitr L. 2015. Insights from the genome of Ophiocordyceps polyrhachis-furcata to pathogenicity and host specificity in insect fungi. BMC Genomics **16**:881. DOI: https://doi.org/10.1186/s12864-015-2101-4

Xu R, Lou Y, Tidu A, Bulet P, Heinekamp T, Martin F, Brakhage A, Li Z, Liégeois S, Ferrandon D. 2023. The Toll pathway mediates Drosophila resilience to Aspergillus mycotoxins through specific Bomanins. EMBO reports **24**:e56036. DOI: https://doi.org/10.15252/embr.202256036

Yassine H, Kamareddine L, Osta MA. 2012. The mosquito melanization response is implicated in defense against the entomopathogenic fungus Beauveria bassiana. PLoS Pathogens **8**:e1003029. DOI: https://doi.org/10.1371/journal.ppat.1003029

Yuan Y, Huang W, Chen K, Ling E. 2020. Beauveria bassiana ribotoxin inhibits insect immunity

1226 responses to facilitate infection via host translational blockage. Developmental & Comparative
1227 Immunology **106**:103605. DOI: https://doi.org/10.1016/j.dci.2019.103605
1228
1229

Figure Legends

Figure 1. Contribution of the four main immune modules to survival upon natural infection with the five fungi. (A-E) Survival rate of male wild-type and deficient flies following infection with the five different fungi shows that *spz*^{rm7} flies (P<0.0001) and *PPO1*$^{\Delta}$, *PPO2*$^{\Delta}$ flies (P<0.0001) are severely affected in their capacity to survive infection with the five fungi compared to wild-type flies. (F) Flies that are devoid of all the four immune modules (*⊿ITPM*) have a significantly shorter lifespan (χ^2=78.50, P<0.0001). Insects treated with 0.05% Tween 80 were used as mock controls. Data were analyzed by Log-rank test and values are pooled from at least three independent experiments. Full statistical details are available on Table S3.

Figure 2. Contribution of the four main immune modules to survival upon septic infection with the five fungi. (**A-C**) Survival rate of male wild-type and deficient flies following pricking with spore suspensions show that *spz*^{rm7} flies (P<0.0001) contribute most to surviving infection by the *B. bassiana*, *M. anisopliae*, and *M. rileyi* as that of natural infection. (**D**) Survival rate of male wild-type and deficient flies following pricking with spore suspensions show that *spz*^{rm7} and to a lower extent *Rel*^{E20} flies exhibited a strong susceptibility to infection with *A. fumigatus* (P<0.0001). (**E**) No significant difference in survival of the four main modules upon infection with *E. muscae* by the injection of protoplasts compared to wild-type flies. (**F**) Survival rate of male flies following injury with a clean needle show that *PPO1*$^{\Delta}$, *PPO2*$^{\Delta}$ flies are severely affected in their capacity to survive wounding compared to wild-type flies (χ^2=20.30, P<0.0001). There was no significant difference in survival of *⊿ITPM* flies upon injection with *E. muscae* protoplasts and injury with a clean needle (χ^2=2.045, P=0.1527). Data were analyzed by Log-rank test and values are pooled from at least three independent experiments. Full statistical details are available on Table S3.

Figure 3. The induction of the Toll pathway in wild-type flies upon infection with the five fungi.

(**A-E**) Expression of *Drosomycin* (*Drs*) in wild-type flies upon natural infection with the five fungi. Shown are the relative expression levels of *Drs* in relation to Rp49. *B. bassiana*, *M. anisopliae* and *M. rileyi* induced relatively high *Drs* expression (compare Y axis to F). *A. fumigatus* did not induce *Drs* expression, while *E. muscae* induced a low *Drs* expression level. (**F**) A high induction of *Drs* was observed in unchallenged flies and flies 48 h after natural infection with *E. muscae* upon septic injury with the Gram-positive bacterium *M. luteus*. UC = Unchallenged, CI = Clean Injury, EM = naturally-infected with *E. muscae;* (**G**) Stronger GFP signal intensity was observed in flies carrying the *Drs-GFP* reporter gene upon natural infection with *B. bassiana* than that with *E. muscae*. (**H**) Kinetic analysis of Toll pathway activity was monitored using unchallenged *Drs-GFP* flies and flies 48 h after natural infection with *E. muscae* upon septic injury with the Gram-positive bacterium *M. luteus.* (**I**) Septic injury with *B. bassiana* spores induced higher *Drs* expression than natural infection (Compare I to A). UC = Unchallenged, CI = Clean injection, Bb = *B.*

bassiana infection (**J**) Injection with *E. muscae* protoplasts did not induce *Drs* expression (Compare J to E). UC = Unchallenged, PBS = Sterile injection, Em = *E. muscae* injection. (**K**) Stronger GFP intensity was observed in flies carrying the *Drs-GFP* reporter gene upon septic infection with *B. bassiana* than that with *E. muscae*. Expression was normalized with w^{1118} UC set as a value of 1. Data were analyzed using One-Way ANOVA followed by Tukey's multiple comparison tests. Values represent the mean ± s.d. of at least three independent experiments. ns, P>0.05, *, P<0.05; **, P<0.01; ***, P<0.001. Full statistical details are available on Table S3.

Figure 4. Morphological development of *E. muscae in vitro* culture and in flies. (**A**) The morphological development of *E. muscae* protoplasts in Grace's Insect Medium showed that round protoplast sprouted and extended to grow at the site of vesicles to form hyphae. Calcofluor White M2R staining showed that cell wall is only present when protoplasts have transformed to hyphae. V: vesicle. (**B**) Five infection stages of *E. muscae* were defined based on the morphological change of flies after infection. Red arrows indicate the white abdomen. (**C**) Calcofluor White M2R staining showed the presence of cell wall of spores contacting with host cuticle (S1), the absence of cell wall of protoplasts (S2), and the presence of thin cell wall when protoplasts transformed to invasive hyphae at S3-S4 and hyphae S5. Red arrows indicate the presence of vesicle in protoplasts and hyphae. C: cuticle; White arrows indicate the primary conidia produced at the tip of the hyphae that extrude from the cadavers.

Figure 5. Contribution of the Psh and GNBP3 to Toll pathway activation. (**A**) A model of GNBP3 and SPs regulating the Toll pathway and the Melanization reaction upon fungal infections. (**B-E**) Natural infection with *B. bassiana*, *M. anisopliae*, and *M. rileyi* revealed that psh^{SK1} flies have a reduced survival rate compared to $GNBP3^{hades}/Df\ (ED4421)$, $modSP^{1}$ and wild-type flies (P<0.0001). $modSP^{1}$ flies were as susceptible to *E. muscae* as spz^{rm7} and psh^{1} flies (P>0.05). The Hayan-psh^{Def} double mutant flies is more susceptible to *B. bassiana*, *M. anisopliae* and *M. rileyi* than psh^{SK1} (Bb, χ^2=36.19, P<0.0001; Ma, χ^2=16.91, P<0.0001; Mr, χ^2=14.14, P=0.0002). Likewise, the double mutant flies *psh;;modSP* were more susceptible to *B. bassiana*, *M. anisopliae* and *M. rileyi* than psh^{SK1} (Bb, χ^2=14.65, P=0.0001; Ma, χ^2=54.88, P<0.0001; Mr, χ^2=22.68, P<0.0001) and $modSP^{1}$ (Bb, χ^2=173.1, P<0.0001; Ma, χ^2=120.6, P<0.0001; Mr, χ^2=55.81, P<0.0001). (**F**) Expression of *Drs* revealed that $GNBP3^{hades}$ flies have wild-type *Drs* expression levels (p>0.05). The Toll pathway was not activated in psh^{SK1} flies as in spz^{rm7}, psh^{1} and *Hayan-psh* ^{Def} flies, and displayed a lower induction in $modSP^{1}$ flies compared to wild-type flies. (**G**) Expression of *BomBc3* showed similar results to the expression of *Drs*. The spz^{rm7} flies as a positive control. Survival tests were analyzed by Log-rank test and gene expression data were analyzed using One-Way ANOVA followed by Tukey's multiples comparison tests. Values represent the mean ± s.d. of at least three independent experiments. Full statistical details are available on Table S3.

1318 **Figure 6. Higher fungal persistence in flies deficient for the Toll pathway**. (**A-C**)
1319 Quantification of fungal loads by qPCR analyses reveals higher fungal loads in *spz*^{rm7}
1320 flies compared to wild-type flies after natural infection with *B. bassiana*, *M.*
1321 *anisopliae* and *E. muscae*. (**D-E**) Higher proportion of flies with GFP and a stronger
1322 GFP intensity were observed in *spz*^{rm7} flies compared to wild-type flies at 48, 72 and
1323 96 hours after pricking with spores of a *M. anisopliae* tagged GFP strain. ns, P>0.05,
1324 **, P<0.01; ****, P<0.0001. Full statistical details are available on Table S3.
1325
1326 **Figure 7. Contribution of host defense peptides and Serine Proteases involved in**
1327 **melanization to survival upon fungal infection.** (**A**) The Bomanin and Daisho1/2
1328 are critical for defense against *B. bassiana*, *M. anisopliae*, *M. rileyi* and *E. muscae*
1329 infection. (**B**) PPO2 mutant flies were more susceptible to fungal infection than PPO1.
1330 The *spz*^{rm7} flies as a positive control. Shown are the median survival for infection with
1331 *B. bassiana*, *M. anisopliae* and *E. muscae*, and cumulative survival for infection with
1332 *M. rileyi*. Data were analyzed using the Log rank test. ns, P>0.05; *, p<0.05; ***,
1333 P<0.001; ****, P<0.0001. Full statistical details are available on Table S3.
1334
1335 **Figure 8. Melanization limits fungal growth.** (**A**) *B. bassiana* fungal load increases
1336 in wild-type and mutants before mortality upon natural infection. *spz*^{rm7} and *PPO1*$^{\triangle}$,
1337 *PPO2*$^{\triangle}$ flies have a higher fungal persistence in *PPO1*$^{\triangle}$, *PPO2*$^{\triangle}$ flies. (**B**) *M.*
1338 *anisopliae* fungal load increases in wild-type and mutants showing similar trends as *B.*
1339 *bassiana* fungal load upon natural infection. Data were analyzed using One-Way
1340 ANOVA followed by Tukey's multiples comparison tests and values are pooled data
1341 from three independent experiments. (**C**) Stronger GFP intensity and faster fungal
1342 dissemination was observed in *spz*^{rm7} and *PPO1*$^{\triangle}$, *PPO2*$^{\triangle}$ flies upon pricking with
1343 spores of a *M. anisopliae* tagged GFP strain. Red arrow indicates the growth of
1344 hyphae at the melanization spot of the pricking site. Full statistical details are
1345 available on Table S3.
1346

1347 # Supplementary Figure Legends

1348

1349 **Figure S1: Contribution of the cellular response to host defense to fungal**
1350 **infection. (A-D)** Survival analysis of males lacking most plasmatocytes—due to Bax
1351 overexpression in plasmatocytes (*Hml Δ-GAL4, UAS-GFP / UAS-Bax*) (Defaye et al.,
1352 2009)—shows only a modest reduction in their ability to survive natural or septic
1353 injury infection with *B. bassiana* and *M. anisopliae*. Given the numerous roles of
1354 hemocytes in immunity and metabolism (Westlake et al., 2024b), these experiments
1355 cannot disentangle the specific contribution of hemocytes to antifungal defense. Both
1356 systemic and natural infections were carried out at 25 °C. $Bom^{\Delta 55C}$ flies were included
1357 as a positive control. (**E**). Spores of *M. anisopliae-GFP* bind to wild-type but not
1358 $NimC1^{1}$;$eater^{1}$ deficient plasmatocyte (stained in red with phalloidin). Plasmatocytes
1359 from third instar larvae were incubated in presence of *M. anisopliae-GFP* for 2 hours.
1360 Representative image are shown. (**F**) $NimC1^{1}$;$eater^{1}$ deficient plasmatocytes display
1361 reduced ability to phagocyte or bind to spores of *M. anisopliae.* Plasmatocytes from
1362 third instar larvae were incubated in presence of *M. anisopliae-GFP* or bead of *S.*
1363 *aureus* for 2 hours. Note that this assay does not allow to distinguish if plasmatocytes
1364 bind to spores or uptake it internally.

1365

1366 **Figure S2. Survival of the female wild-type and mutant flies deficient for the four**
1367 **main immune modules upon natural infection with the five fungi.** (**A-E**) Survival
1368 rate of the females shows that spz^{rm7} flies (P<0.0001) and *PPO1, PPO2* double mutant
1369 flies (P<0.0001) are severely affected in their capacity to survive infection with the
1370 five fungi compared to wild-type w^{1118} flies. (**F**) The evaluation of spore concentration
1371 after the 24 h ejection from the fresh cadavers shows that more spores were produced
1372 from female cadavers than male cadavers (**, P<0.01). For natural infection of *E.*
1373 *muscae*, a total of 10 female and 10 male fresh cadavers were used for one infection
1374 treatment by spore shower. Data were analyzed using the Log rank test and values are
1375 pooled data from at least three independent experiments. Full statistical details are
1376 available on Table S3. Related to Figure 1.

1377

1378 **Figure S3. Survival of the female wild-type and mutants devoid of the four main**
1379 **immune modules upon septic infection with the five fungi.** (**A-C**) Survival rate of
1380 females following pricking with spore suspensions show that spz^{rm7} flies (P<0.0001)
1381 contribute most to surviving infection by the *B. bassiana*, *M. anisopliae*, and *M. rileyi*.
1382 (**D**) spz^{rm7} and to lower extent Rel^{E20} females exhibited a strong susceptibility to
1383 infection with *A. fumigatus* (P<0.0001). (**E**) No significant difference in survival of
1384 the four main modules upon infection with *E. muscae* by the injection of protoplasts
1385 compared to wild-type females. (**F**) Survival of w^{1118} flies upon infection with *E.*
1386 *muscae* showed that faster killing was found when injected with a higher
1387 concentration of protoplasts (****, P<0.0001). Data were analyzed using the Log
1388 rank test and values are pooled data from at least three independent experiments. Full
1389 statistical details are available on Table S3. Related to Figure 2.

1390

1391 **Figure S4. Expression of Bomanin (*BomBc3*) in wild-type flies upon infection**
1392 **with the five fungi.** (**A-C**) Natural infection with *M. anisopliae* induced a highest
1393 expression of *BomBc3,* followed by *B. bassiana* and *M. rileyi* only induced the
1394 expression of *BomBc3* at a late stage, at 120 h after infection. (**D**) Natural infection
1395 with *A.fumigatus* could not induce the expression of *BomBc3.* (**E**) Natural infection
1396 with *E. muscae* induced a low expression of *BomBc3* at 24 h and 48 h after infection,
1397 then followed by a significant decrease. (**F**) Septic infection with *B. bassiana* spores
1398 activates higher *BomBc3* expression compared to natural infection and clean injury
1399 with a needle. (**G**) Expression of *BomBc3* after injection with *E. muscae* protoplasts
1400 was similar to the injection with PBS, indicating protoplasts cannot activate Toll
1401 signaling. Expression was normalized with w^{1118} UC set as a value of 1. Data were
1402 analyzed using One-Way ANOVA followed by Tukey's multiple comparison tests. ns,
1403 P>0.05; *, P<0.05; **, P<0.01; ***, P<0.001; ****, P<0.0001. Values represent the
1404 mean ± s.d. of at least three independent experiments. Full statistical details are
1405 available on Table S3. Related to Figure 3.
1406

1407 **Figure S5. DAPI staining of the *E. muscae* protoplasts**.
1408

1409 **Figure S6. Contribution of GNBP3 and GNGP like 3 to survival upon natural**
1410 **infection with *B. bassiana* and *M. anisopliae*.** (**A-B**) Survival rate of male flies
1411 following infection with the two fungi shows that both GNBP3 and GNGP like 3
1412 mutant flies are not susceptible or slightly susceptible to *B. bassiana* and *M.*
1413 *anisopliae*. Full statistical details are available on Table S3. Related to Figure 5.
1414

1415 **Figure S7. Fungal dissemination from wild-type and spz^{rm7} cadavers after natural**
1416 **infection with *M. anisopliae*.** *Metarhizium anisopliae* extruding from cuticle and
1417 growing in spz^{rm7} cadavers are faster than that in wild-type cadavers. *M. anisopliae*
1418 can eventually disseminate through the whole flies both in wild-type and spz^{rm7}
1419 cadavers. Related to Figure 6.
1420

1421 **Figure S8. Sum survival curves of single and compound host defense peptides**
1422 **mutants after infection with *B. bassiana*, *M. anisopliae*, *M. rileyi* and *E. muscae*.**
1423 Full statistical details are available on Table S3. Related to Figure 7.
1424

1425 **Figure S9. Sum survival curves of mutants of SPs involved in melanization after**
1426 **infection with *B. bassiana*, *M. anisopliae*, *M. rileyi* and *E. muscae*.** Full statistical
1427 details are available on Table S3. Related to Figure 7.
1428

1429 **Figure S10. Expression of *Drosomycin* of mutants of SPs involved in melanization**
1430 **upon natural and septic infection with *B. bassiana* and *M. anisopliae*.** (**A-B**)
1431 Statistical analysis reveals higher *Drosomycin* expression in *PPO1, PPO2* double
1432 mutant compared to wild-type at 72 h and 120 h after natural infection with *B.*
1433 *bassiana* and at 72 h after natural infection with *M. anisopliae* (*, P<0.05; ***,

1434 P<0.001). The *spz*^{rm7} flies as a positive control. (**C**) Compared with wild-type flies,
1435 PPO1, PPO2 double mutant flies exhibit an enhanced Toll pathway activity upon
1436 clean injury and septic infection with *M. anisopliae* (ns, P>0.05; *, p<0.05; ***,
1437 P<0.001; ****, P<0.0001). Expression was normalized with *w*^{1118} UC set as a value of
1438 1. Data were analyzed using One-Way ANOVA followed by Tukey's multiple
1439 comparison tests and values represent the mean ± s.d. of at least three independent
1440 experiments. Full statistical details are available on Table S3. Related to Figure 7.

Figure 1

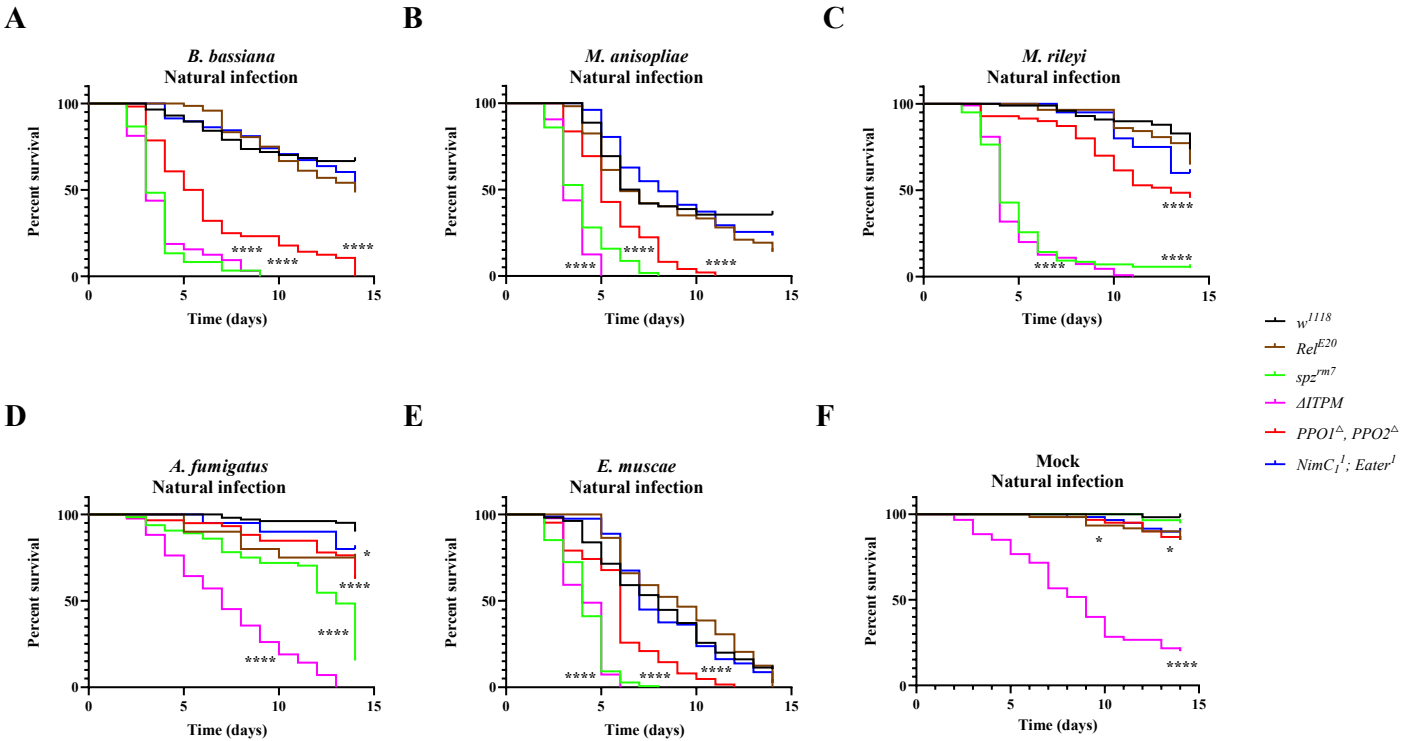
A
B. bassiana
Natural infection
B
M. anisopliae
Natural infection
C
M. rileyi
Natural infection
D
A. fumigatus
Natural infection
E
E. muscae
Natural infection
F
Mock
Natural infection
Percent survival
Time (days)
w1118
RelE20
spzrm7
ΔITPM
PPO1Δ, PPO2Δ
NimC1 1; Eater1

Figure 2

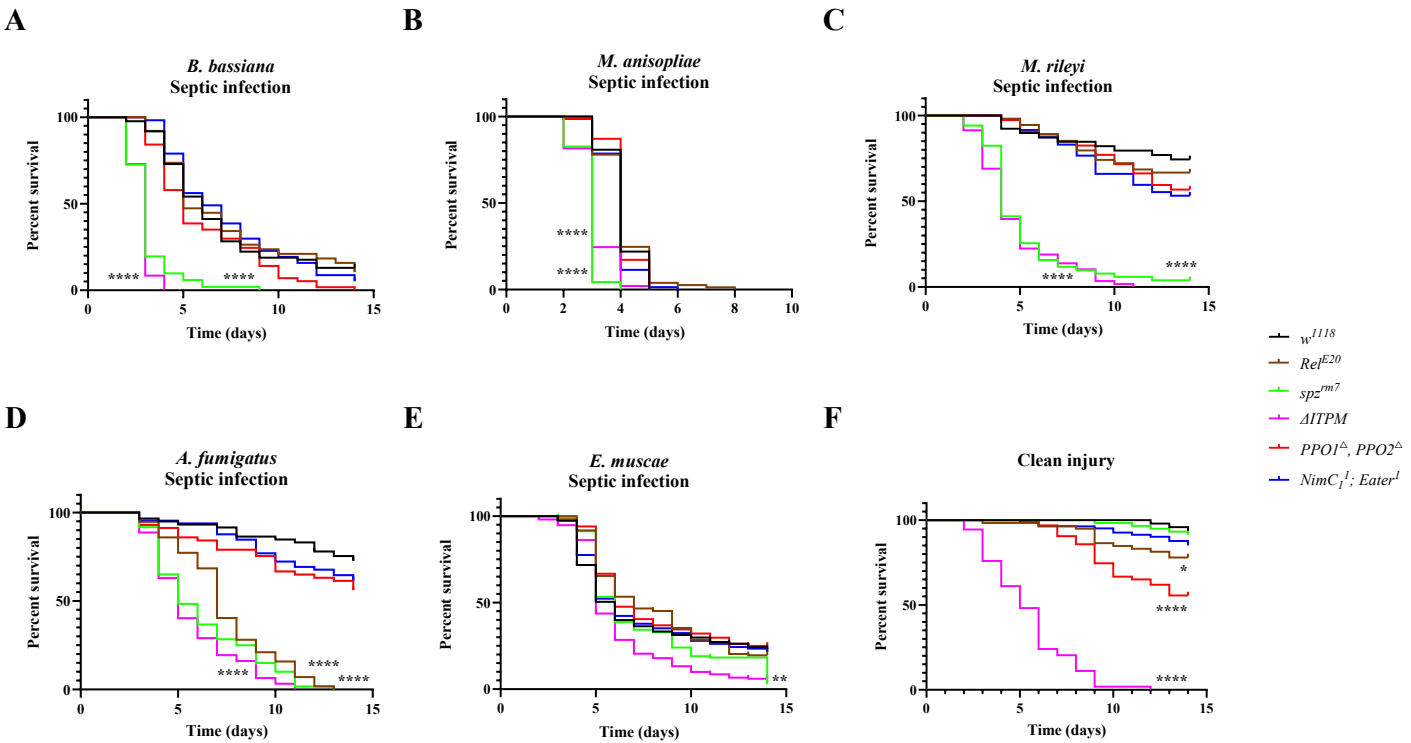
A
B. bassiana
Septic infection
Percent survival
Time (days)
****
****
B
M. anisopliae
Septic infection
Percent survival
Time (days)
****
****
C
M. rileyi
Septic infection
Percent survival
Time (days)
****
****
D
A. fumigatus
Septic infection
Percent survival
Time (days)
****
****
****
E
E. muscae
Septic infection
Percent survival
Time (days)
**
F
Clean injury
Percent survival
Time (days)
*
****
****
w1118
RelE20
spzrm7
ΔITPM
PPO1Δ, PPO2Δ
NimC1 1; Eater1

Figure 3

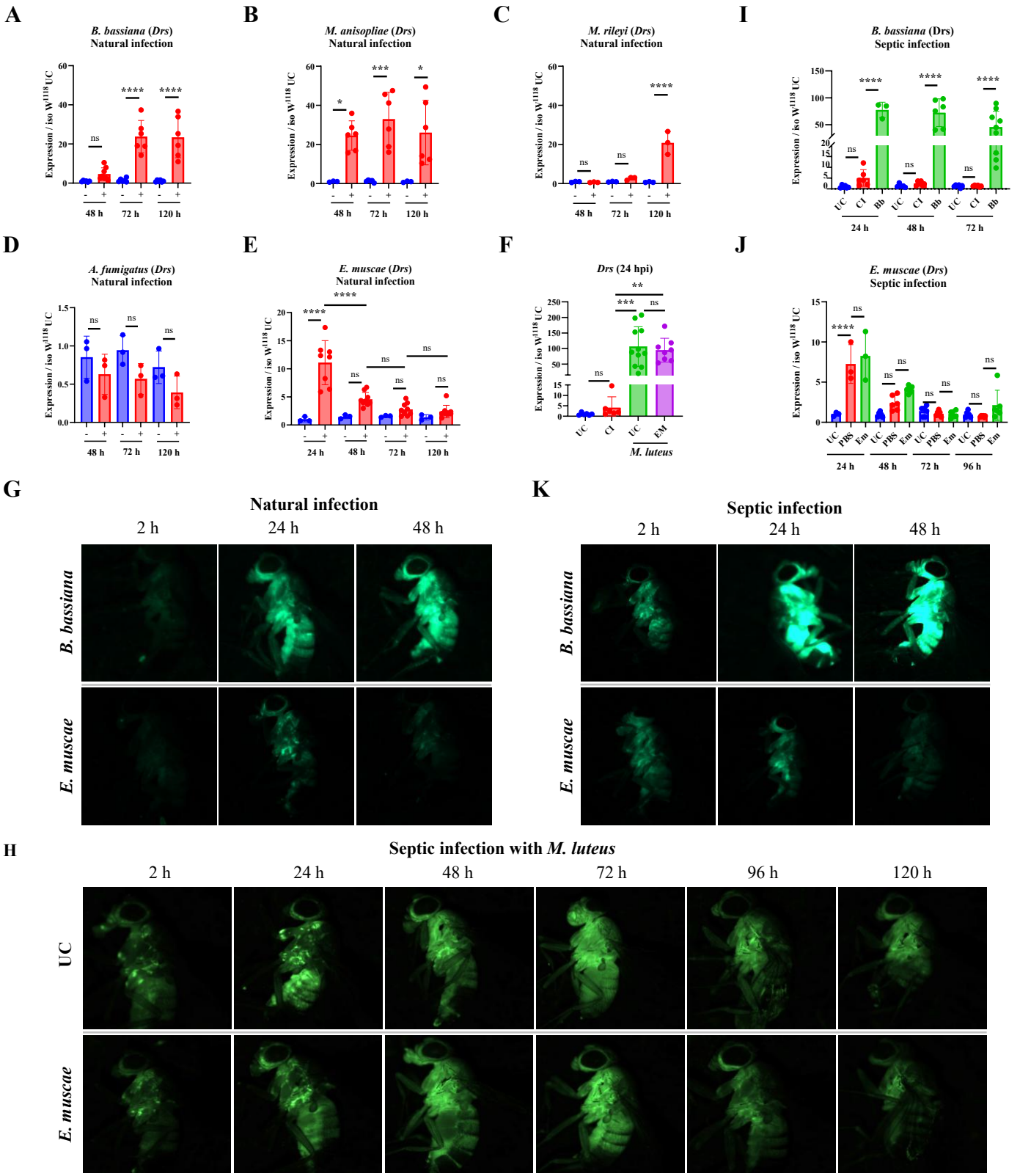
A
B. bassiana (Drs)
Natural infection
Expression / iso W1118 UC
48 h
72 h
120 h
B
M. anisopliae (Drs)
Natural infection
C
M. rileyi (Drs)
Natural infection
I
B. bassiana (Drs)
Septic infection
UC
C1
Bb
24 h
48 h
72 h
D
A. fumigatus (Drs)
Natural infection
E
E. muscae (Drs)
Natural infection
F
Drs (24 hpi)
M. luteus
J
E. muscae (Drs)
Septic infection
PBS
Em
96 h
G
Natural infection
2 h
24 h
48 h
B. bassiana
E. muscae
K
Septic infection
H
Septic infection with M. luteus
72 h
96 h
120 h
UC

Figure 4

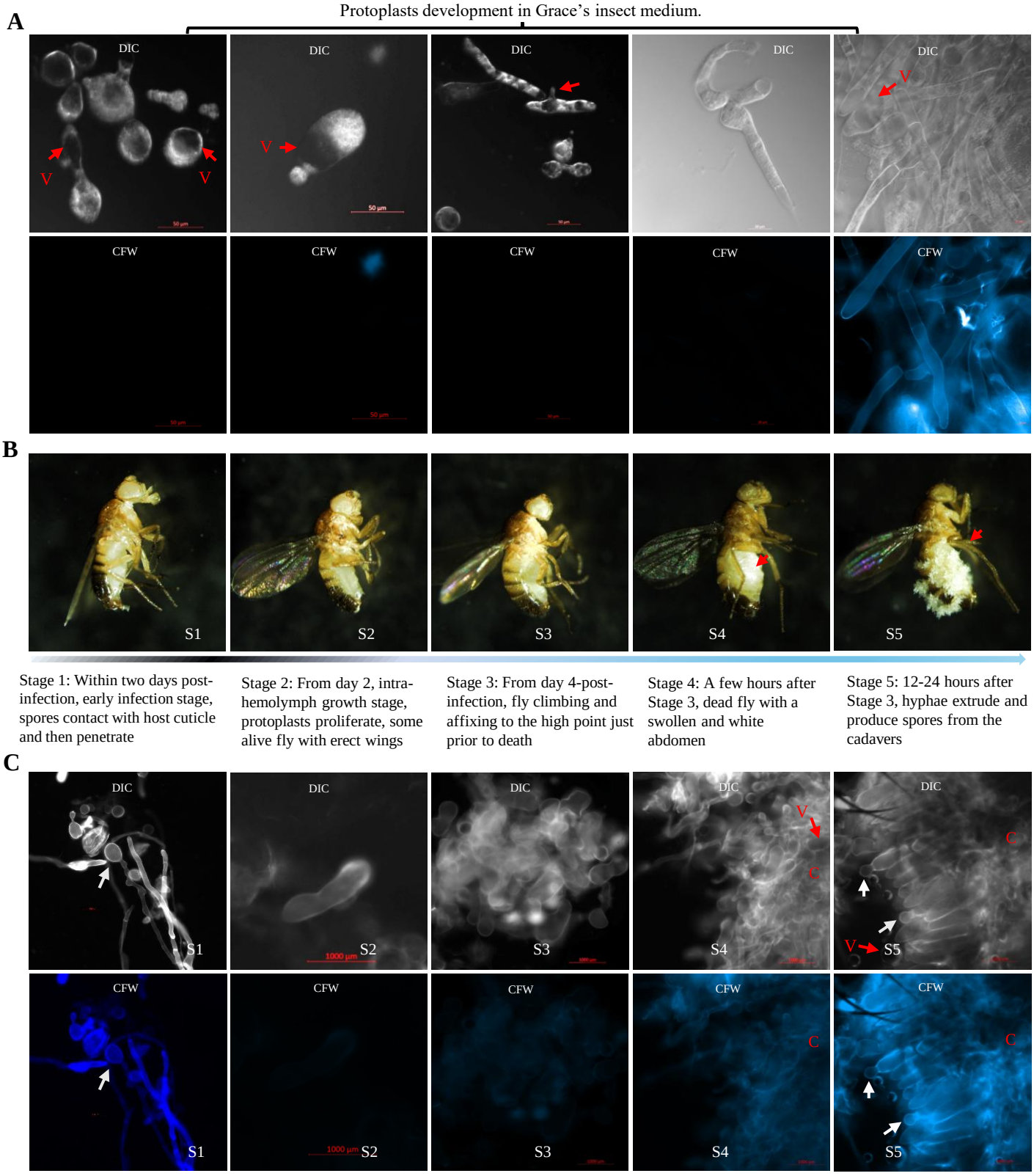
A
Protoplasts development in Grace's insect medium.
DIC
V
CFW
B
S1
S2
S3
S4
S5
Stage 1: Within two days post-infection, early infection stage, spores contact with host cuticle and then penetrate
Stage 2: From day 2, intra-hemolymph growth stage, protoplasts proliferate, some alive fly with erect wings
Stage 3: From day 4-post-infection, fly climbing and affixing to the high point just prior to death
Stage 4: A few hours after Stage 3, dead fly with a swollen and white abdomen
Stage 5: 12-24 hours after Stage 3, hyphae extrude and produce spores from the cadavers
C
C
1000 μm

Figure 5

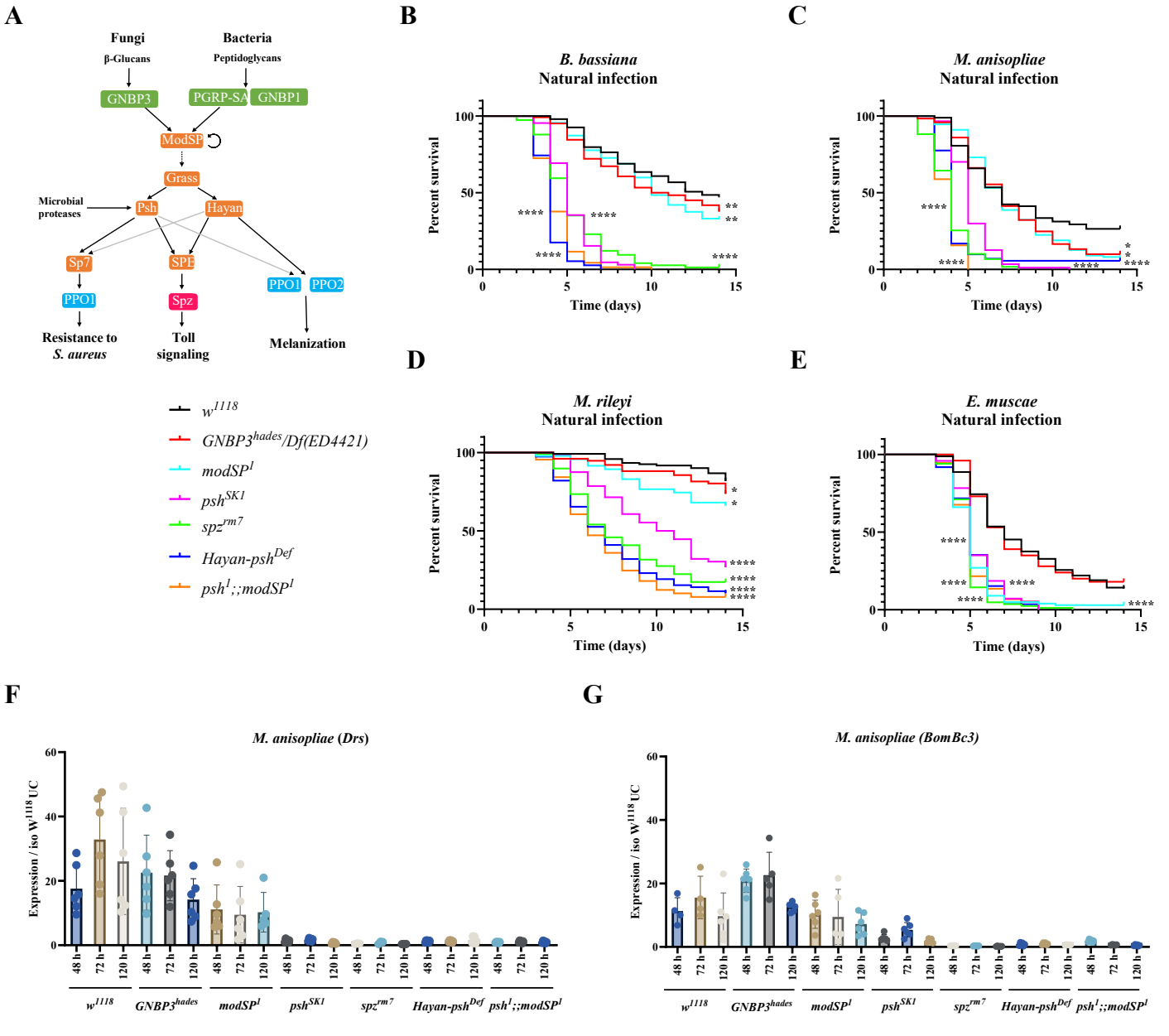
A
Fungi
Bacteria
β-Glucans
Peptidoglycans
GNBP3
PGRP-SA
GNBP1
ModSP
Grass
Microbial proteases
Psh
Hayan
Sp7
SPE
PPO1
PPO2
Spz
Resistance to S. aureus
Toll signaling
Melanization
B
B. bassiana
Natural infection
C
M. anisopliae
Natural infection
D
M. rileyi
Natural infection
E
E. muscae
Natural infection
Percent survival
Time (days)
w1118
GNBP3hades/Df(ED4421)
modSP1
pshSK1
spzrm7
Hayan-pshDef
psh1;;modSP1
F
M. anisopliae (Drs)
G
M. anisopliae (BomBc3)
Expression / iso w1118 UC
48 h
72 h
120 h

Figure 6

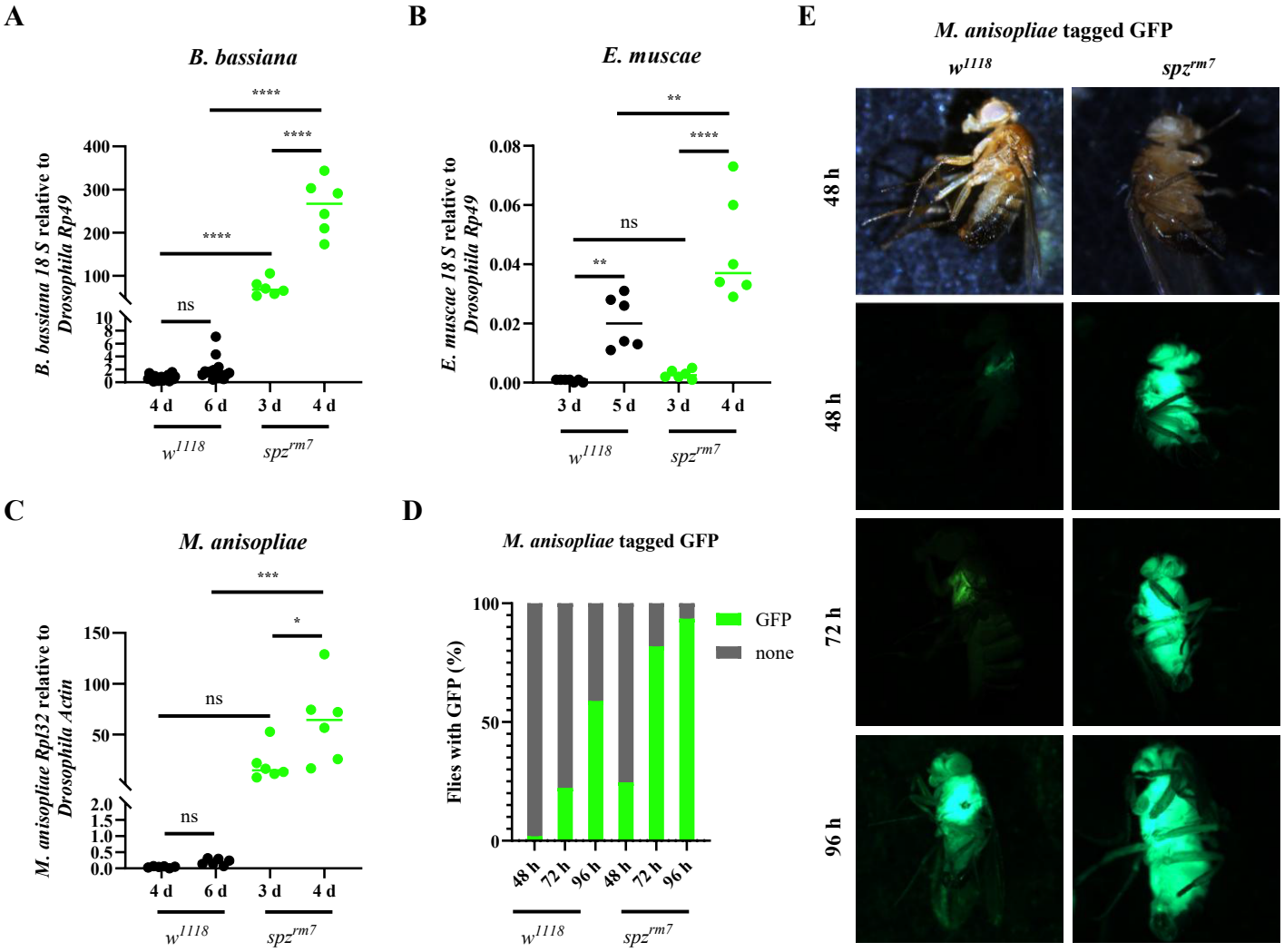
A
B. bassiana
B. bassiana 18 S relative to Drosophila Rp49
400
300
200
100
10
8
6
4
2
0
****
****
ns
4 d
6 d
3 d
4 d
w1118
spzrm7
B
E. muscae
E. muscae 18 S relative to Drosophila Rp49
0.08
0.06
0.04
0.02
0.00
**
****
ns
**
3 d
5 d
3 d
4 d
w1118
spzrm7
C
M. anisopliae
M. anisopliae Rpl32 relative to Drosophila Actin
150
100
50
2.0
1.5
1.0
0.5
0.0
***
*
ns
ns
4 d
6 d
3 d
4 d
w1118
spzrm7
D
M. anisopliae tagged GFP
Flies with GFP (%)
100
50
0
GFP
none
48 h
72 h
96 h
48 h
72 h
96 h
w1118
spzrm7
E
M. anisopliae tagged GFP
w1118
spzrm7
48 h
48 h
72 h
96 h

Figure 7

A

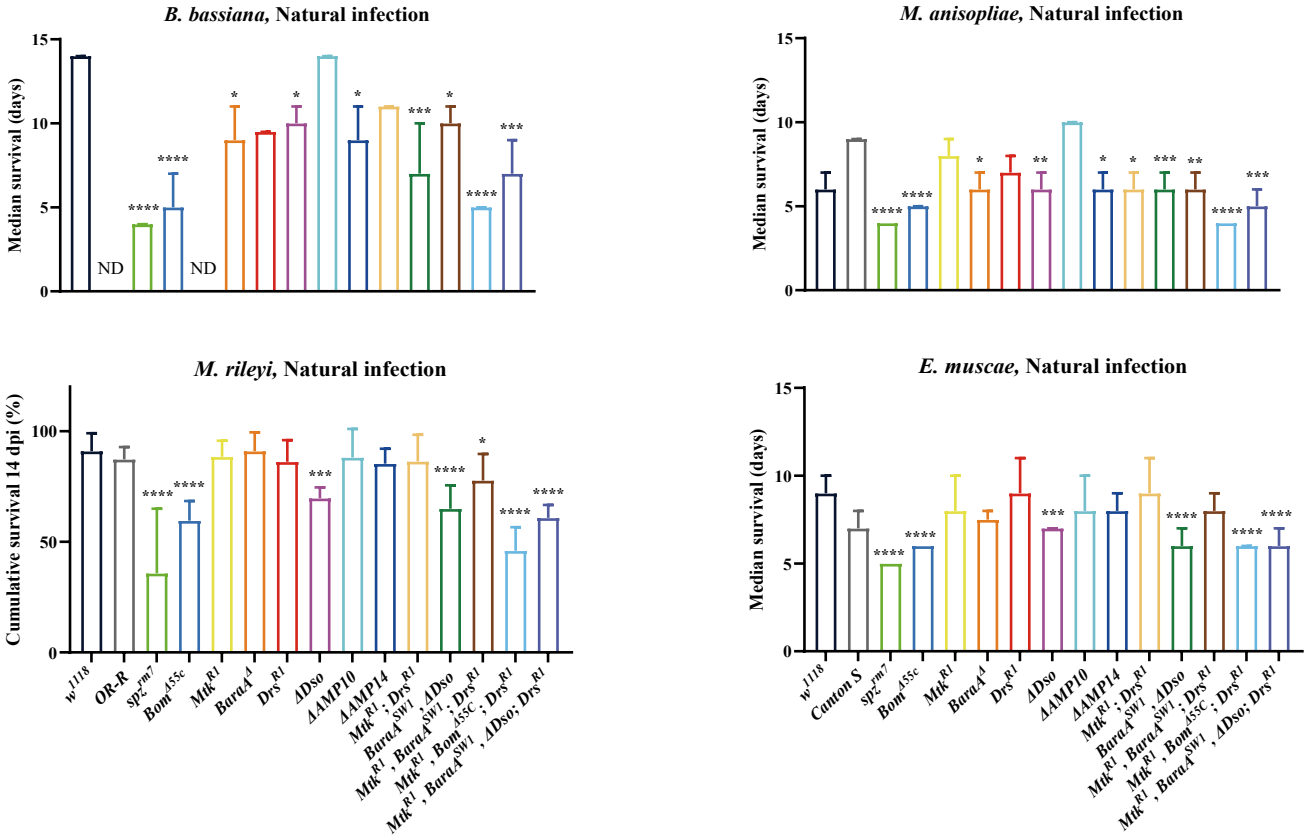
B. bassiana, Natural infection
Median survival (days)
ND
ND
M. anisopliae, Natural infection
Median survival (days)
M. rileyi, Natural infection
Cumulative survival 14 dpi (%)
E. muscae, Natural infection
Median survival (days)
w1118
OR-R
spz rm7
Bom Δ55c
Mtk R1
BaraA 4
Drs R1
ΔDso
ΔAMP10
ΔAMP14
Mtk R1 ; Drs R1
BaraA SW1 ; Drs R1
Mtk R1 , BaraA SW1 , ΔDso
Mtk R1 , Bom Δ55C ; Drs R1
Mtk R1 , BaraA SW1 , ΔDso; Drs R1
Canton S

B

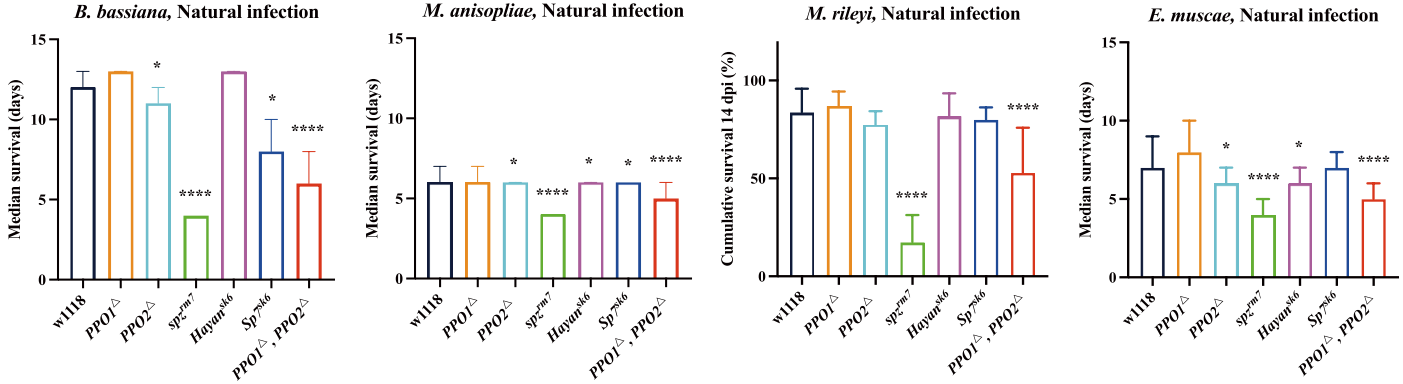
B. bassiana, Natural infection
Median survival (days)
M. anisopliae, Natural infection
Median survival (days)
M. rileyi, Natural infection
Cumulative survival 14 dpi (%)
E. muscae, Natural infection
Median survival (days)
w1118
PPO1Δ
PPO2Δ
spz rm7
Hayan sk6
Sp zsk6
PPO1Δ , PPO2Δ

Figure 8

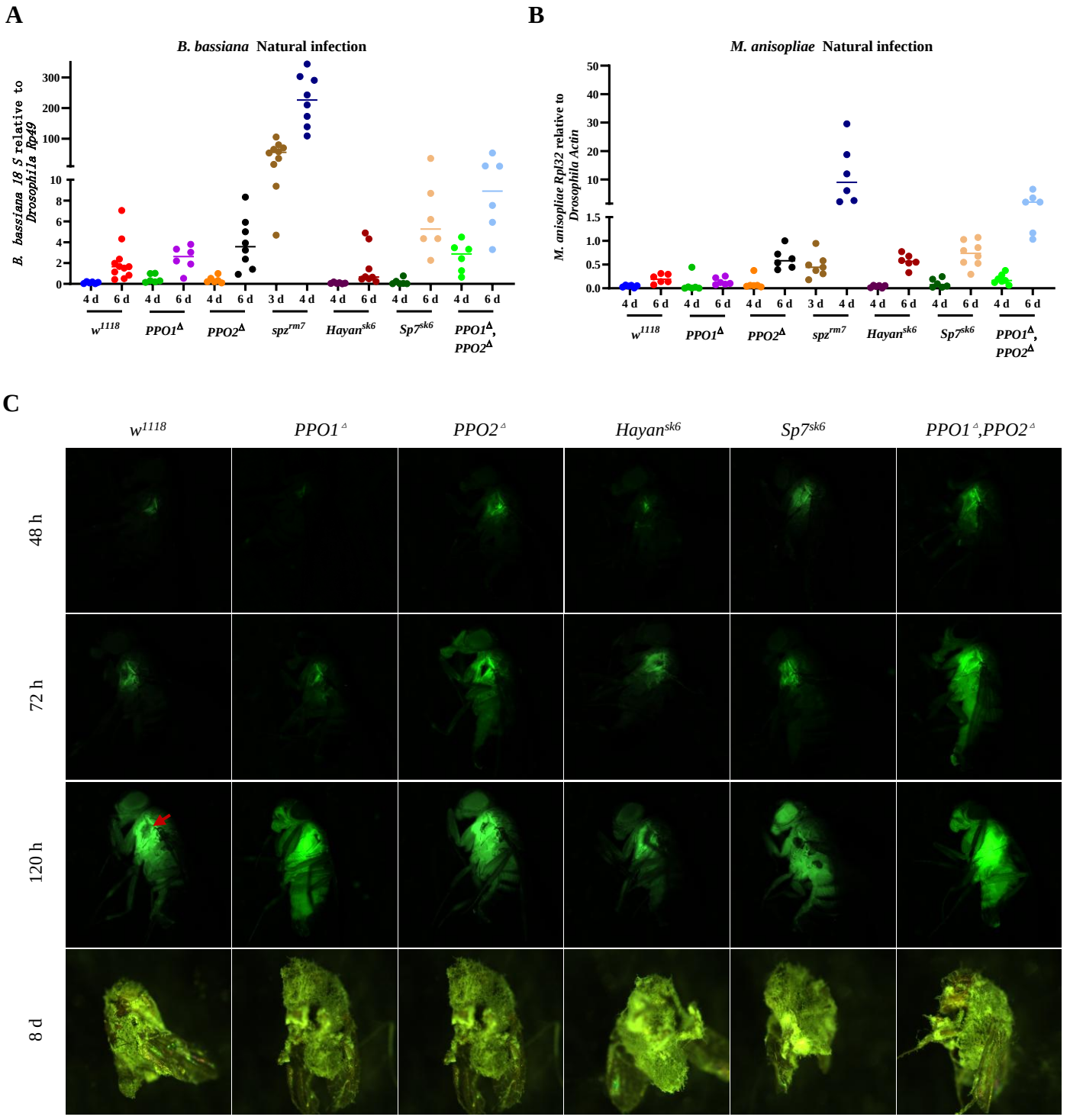
A
B. bassiana Natural infection
B. bassiana 18 S relative to Drosophila Rp49
300
200
100
10
8
6
4
2
0
4 d
6 d
3 d
w1118
PPO1Δ
PPO2Δ
spzrm7
Hayansk6
Sp7sk6
PPO1Δ, PPO2Δ
B
M. anisopliae Natural infection
M. anisopliae Rpl32 relative to Drosophila Actin
50
40
30
20
10
1.5
1.0
0.5
0.0
C
w1118
PPO1Δ
PPO2Δ
Hayansk6
Sp7sk6
PPO1Δ,PPO2Δ
48 h
72 h
120 h
8 d

Figure S1

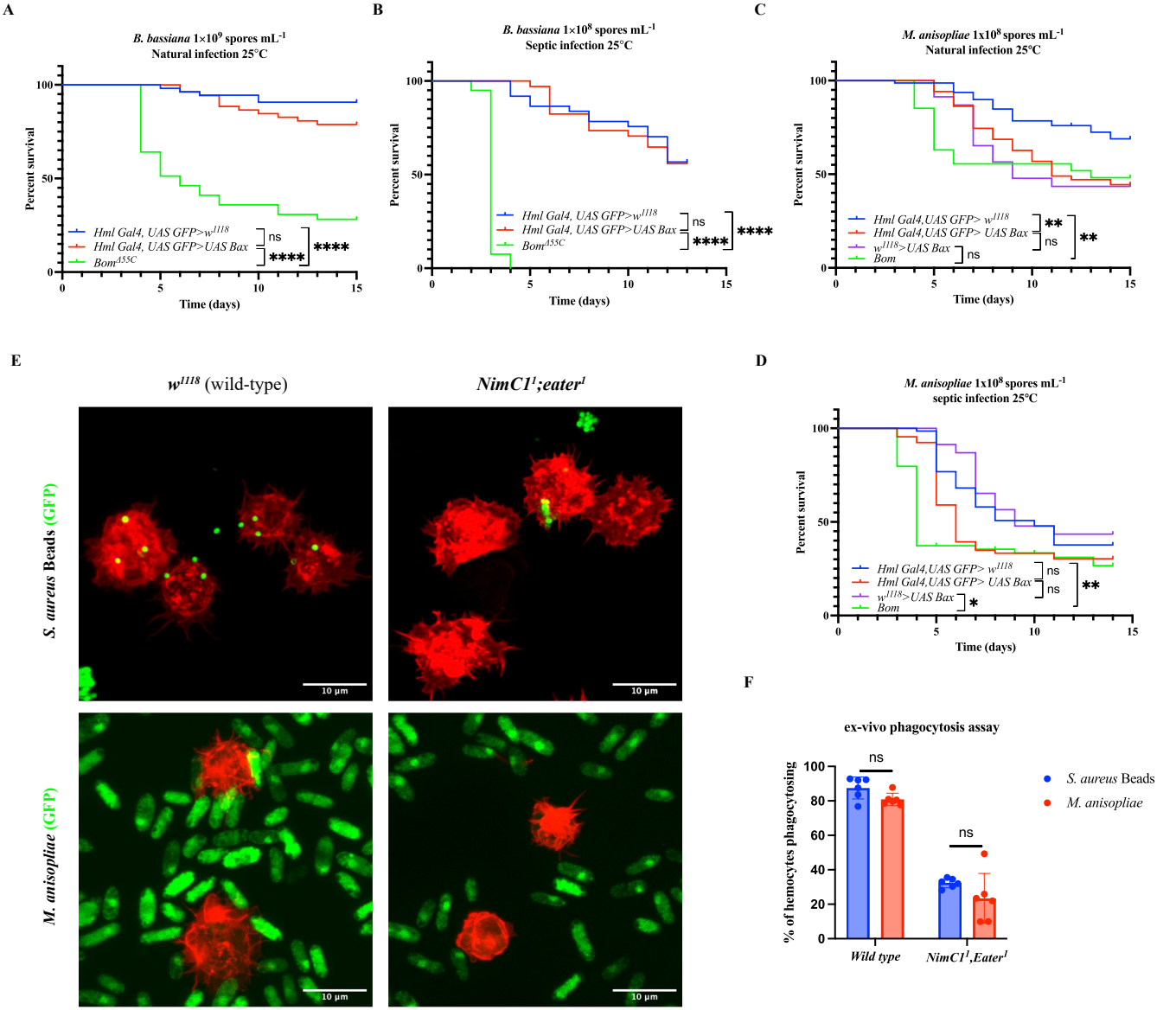
A
B. bassiana 1×10^9 spores mL^-1
Natural infection 25°C
Percent survival
Time (days)
Hml Gal4, UAS GFP>w^1118
Hml Gal4, UAS GFP>UAS Bax
Bom^Δ55C
ns
****
B
B. bassiana 1×10^8 spores mL^-1
Septic infection 25°C
C
M. anisopliae 1x10^8 spores mL^-1
Natural infection 25°C
Hml Gal4,UAS GFP> w^1118
Hml Gal4,UAS GFP> UAS Bax
w^1118>UAS Bax
Bom
**
D
M. anisopliae 1x10^8 spores mL^-1
septic infection 25°C
*
E
w^1118 (wild-type)
NimC1^1;eater^1
S. aureus Beads (GFP)
M. anisopliae (GFP)
10 µm
F
ex-vivo phagocytosis assay
% of hemocytes phagocytosing
Wild type
NimC1^1,Eater^1
S. aureus Beads
M. anisopliae

Figure S2

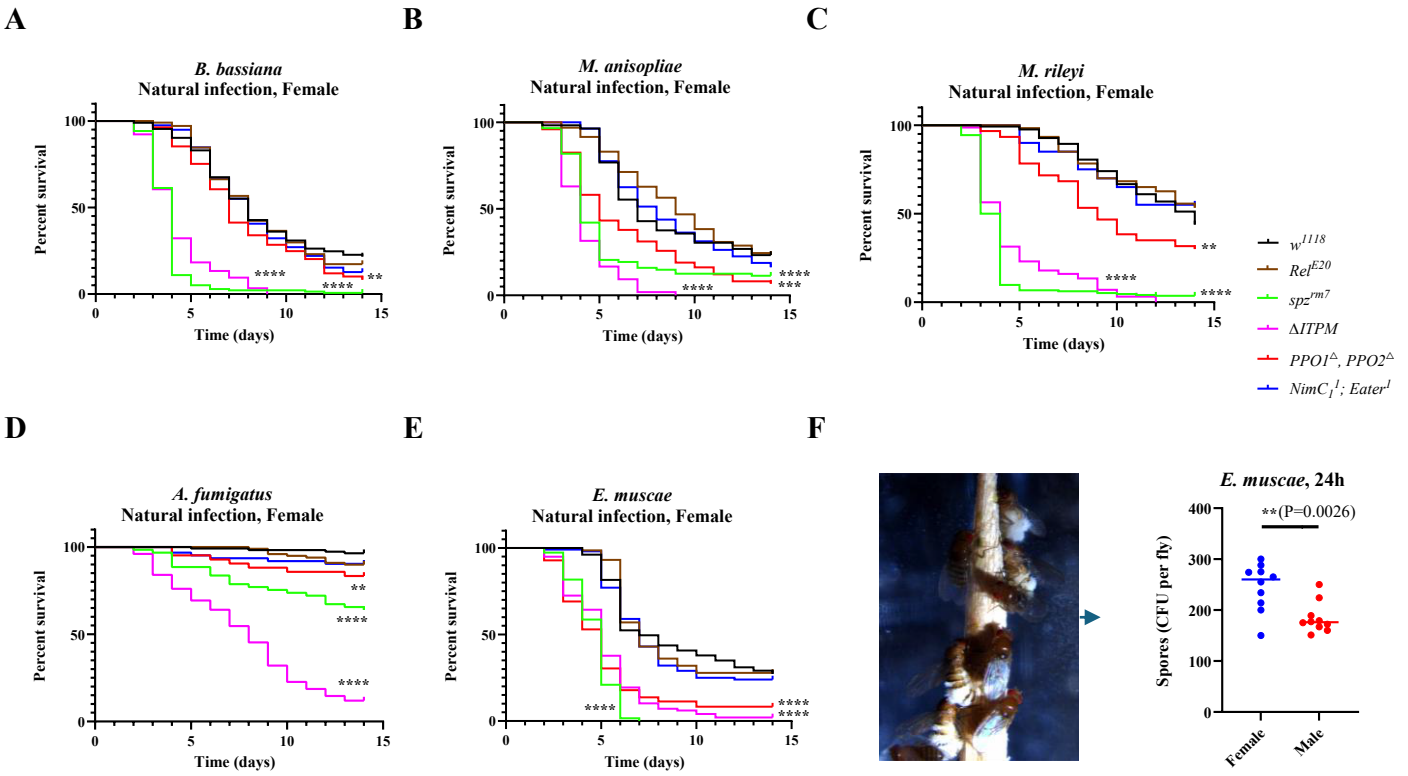
A
B. bassiana
Natural infection, Female
Percent survival
Time (days)
B
M. anisopliae
Natural infection, Female
C
M. rileyi
Natural infection, Female
w1118
Rel E20
spz rm7
ΔITPM
PPO1Δ, PPO2Δ
NimC1 1; Eater1
D
A. fumigatus
Natural infection, Female
E
E. muscae
Natural infection, Female
F
E. muscae, 24h
**(P=0.0026)
Spores (CFU per fly)
Female
Male

Figure S3

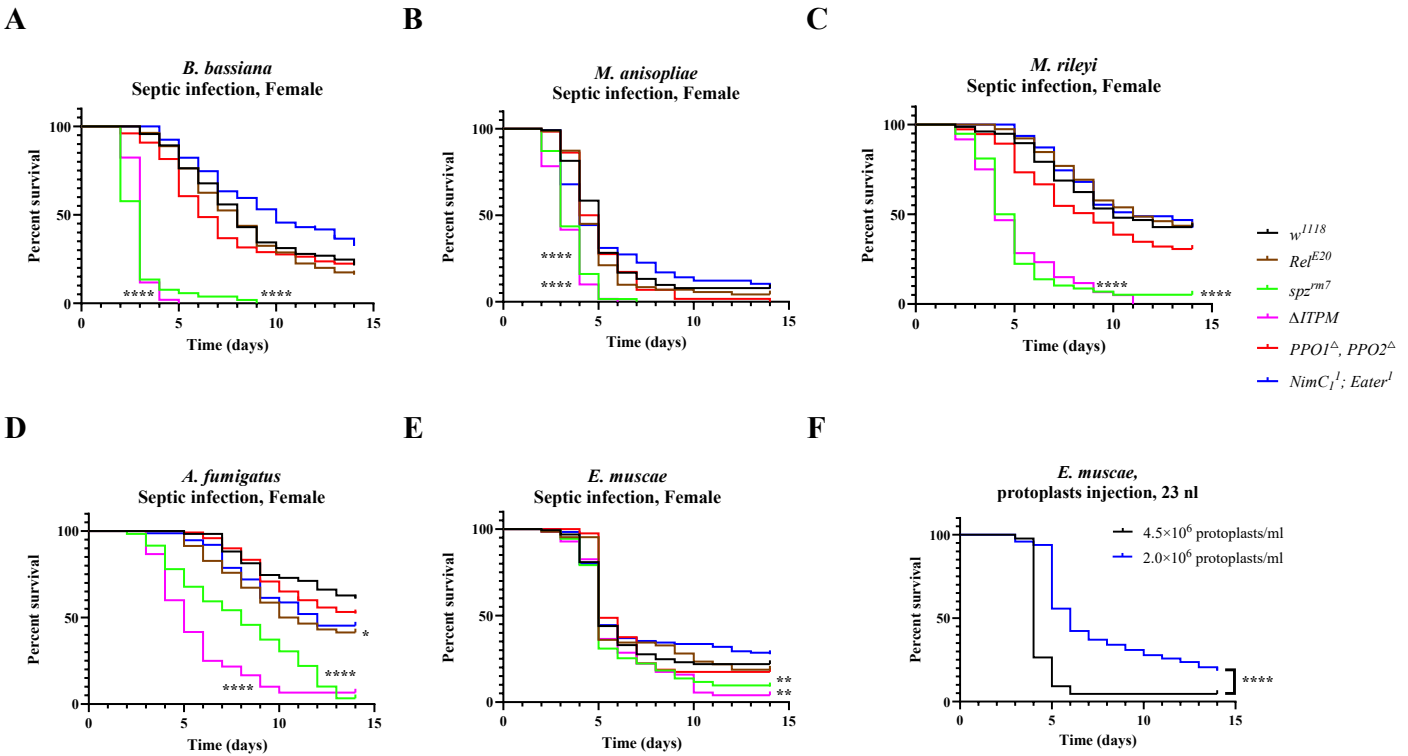
A
B. bassiana
Septic infection, Female
Percent survival
Time (days)
****
****
B
M. anisopliae
Septic infection, Female
Percent survival
Time (days)
****
****
C
M. rileyi
Septic infection, Female
Percent survival
Time (days)
****
****
w1118
Rel E20
spz rm7
ΔITPM
PPO1Δ, PPO2Δ
NimC1 1; Eater 1
D
A. fumigatus
Septic infection, Female
Percent survival
Time (days)
*
****
****
E
E. muscae
Septic infection, Female
Percent survival
Time (days)
**
**
F
E. muscae,
protoplasts injection, 23 nl
4.5×10^6 protoplasts/ml
2.0×10^6 protoplasts/ml
Percent survival
Time (days)
****

Figure S4

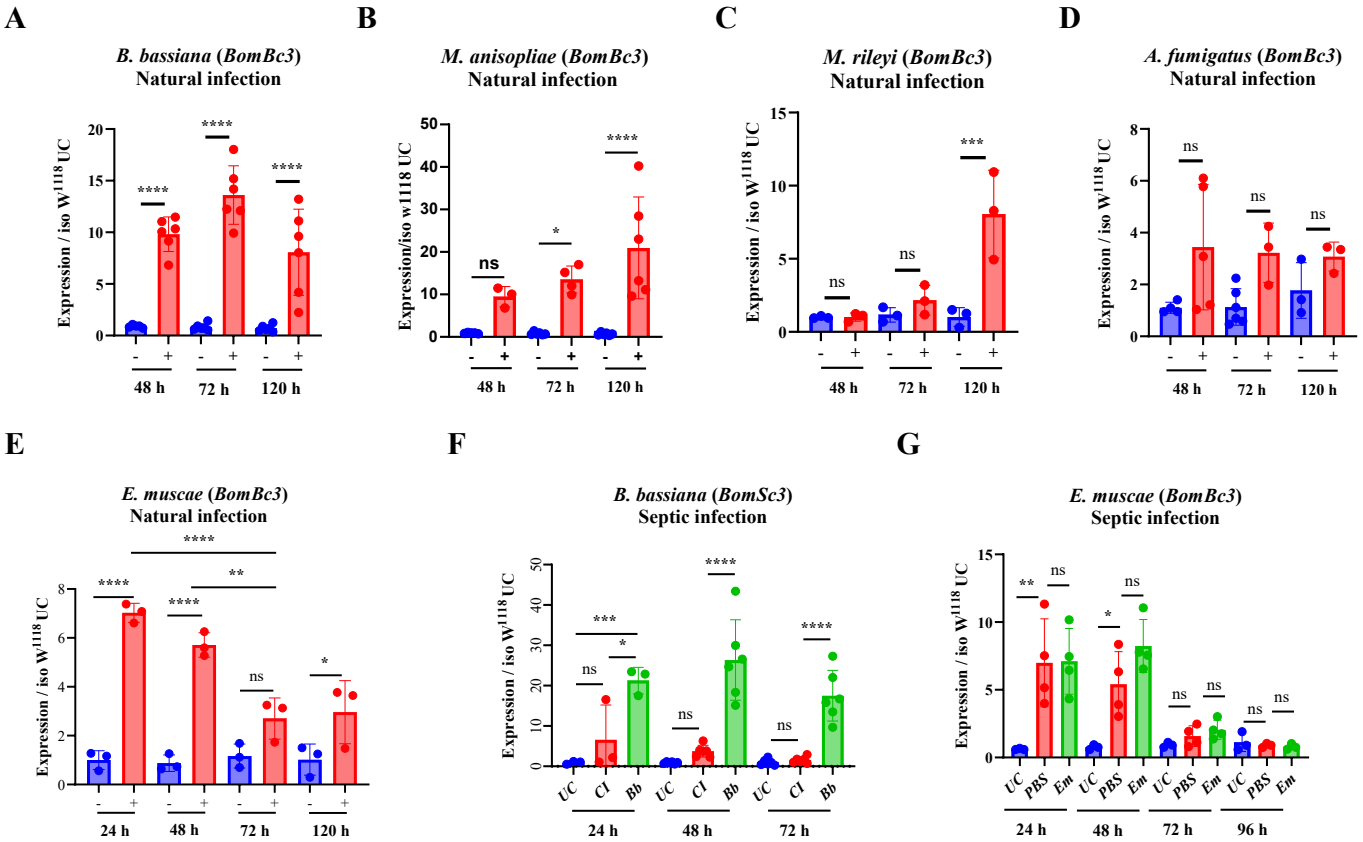
A
B. bassiana (BomBc3)
Natural infection
Expression / iso W1118 UC
48 h
72 h
120 h
B
M. anisopliae (BomBc3)
Natural infection
Expression/iso w1118 UC
C
M. rileyi (BomBc3)
Natural infection
D
A. fumigatus (BomBc3)
Natural infection
E
E. muscae (BomBc3)
Natural infection
24 h
F
B. bassiana (BomSc3)
Septic infection
UC
Cl
Bb
G
E. muscae (BomBc3)
Septic infection
PBS
Em
96 h

Figure S5

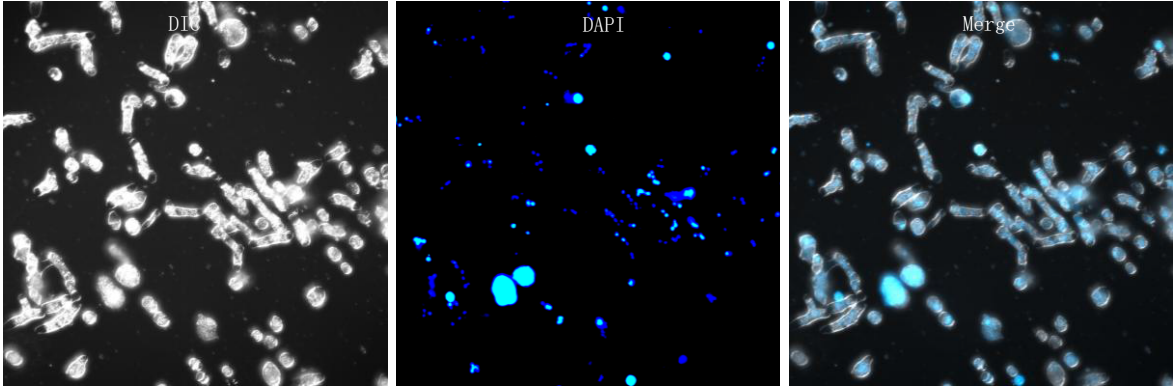

Figure S6

A

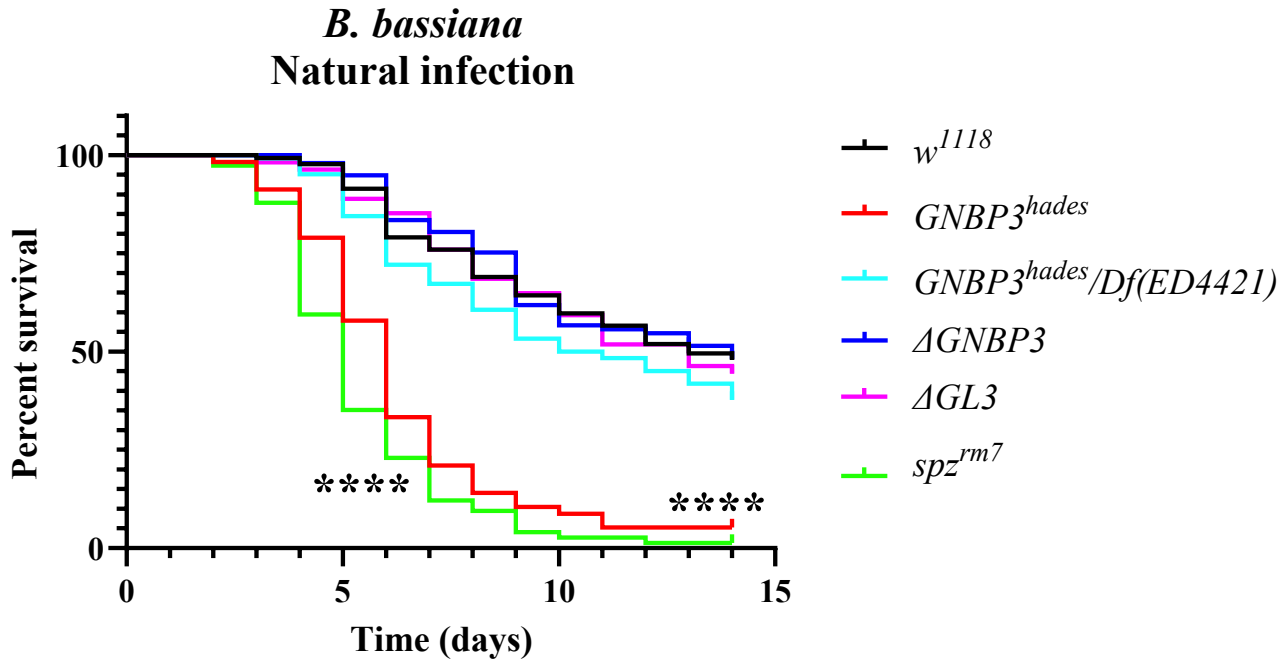
B. bassiana
Natural infection
Percent survival
100
50
0
0
5
10
15
Time (days)
****
****
w1118
GNBP3hades
GNBP3hades/Df(ED4421)
ΔGNBP3
ΔGL3
spzrm7

B

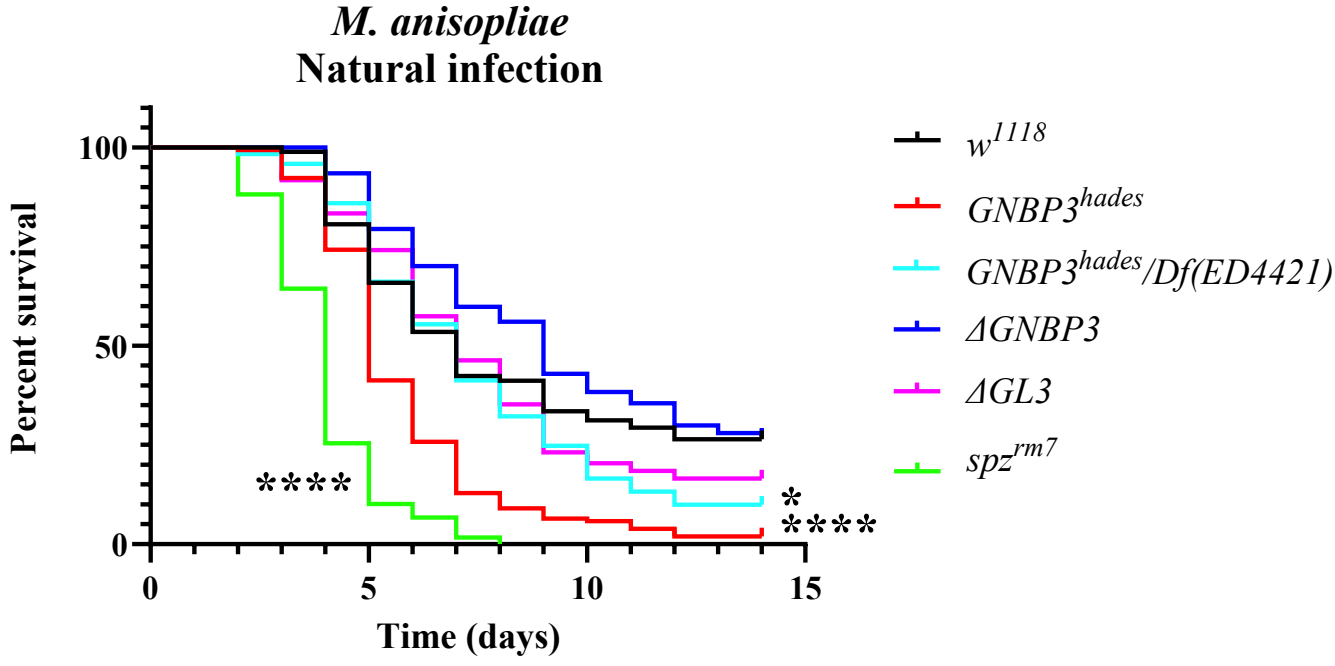
M. anisopliae
Natural infection
Percent survival
100
50
0
0
5
10
15
Time (days)
****
*
****
w1118
GNBP3hades
GNBP3hades/Df(ED4421)
ΔGNBP3
ΔGL3
spzrm7

Figure S7

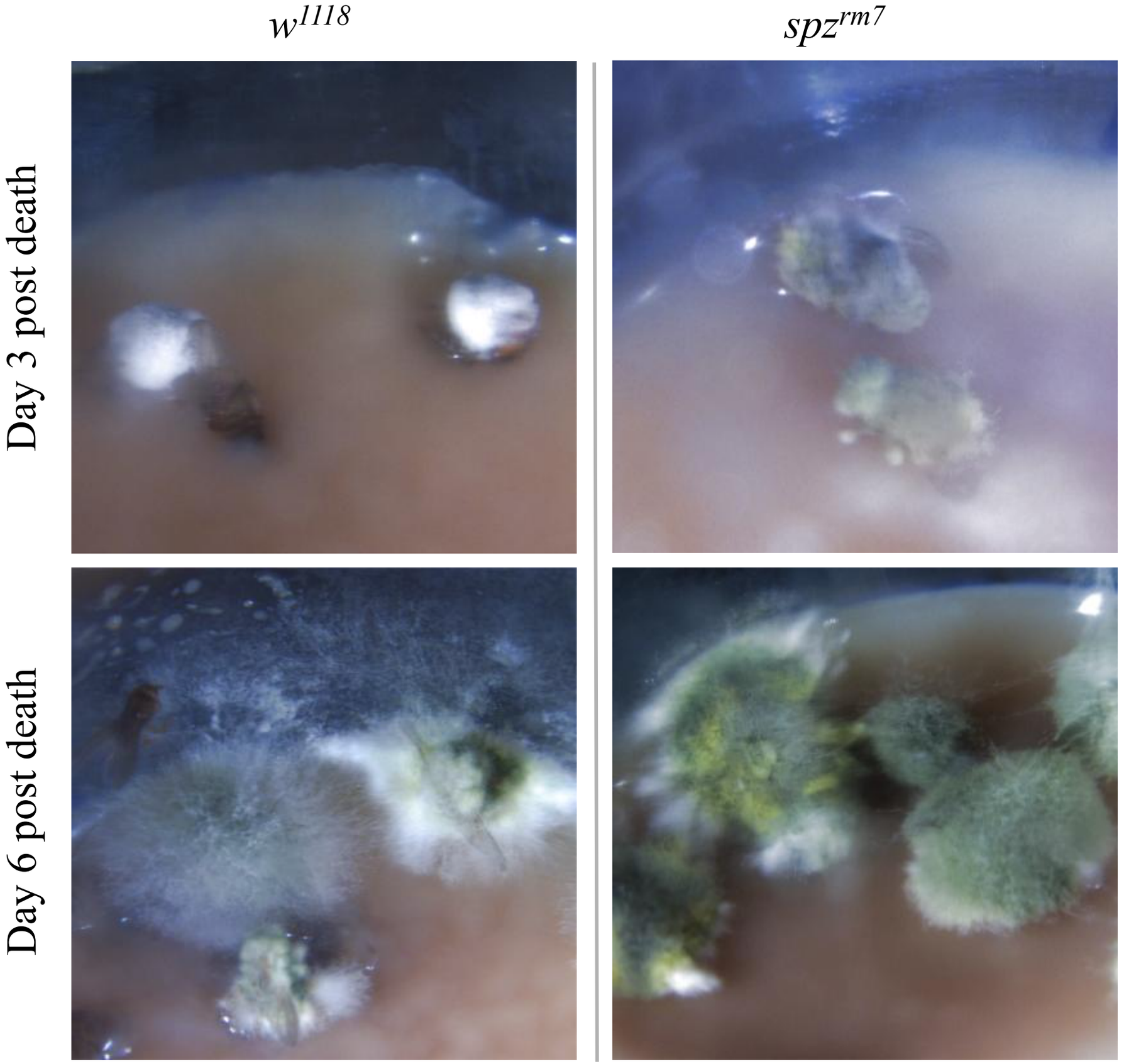

Figure S8

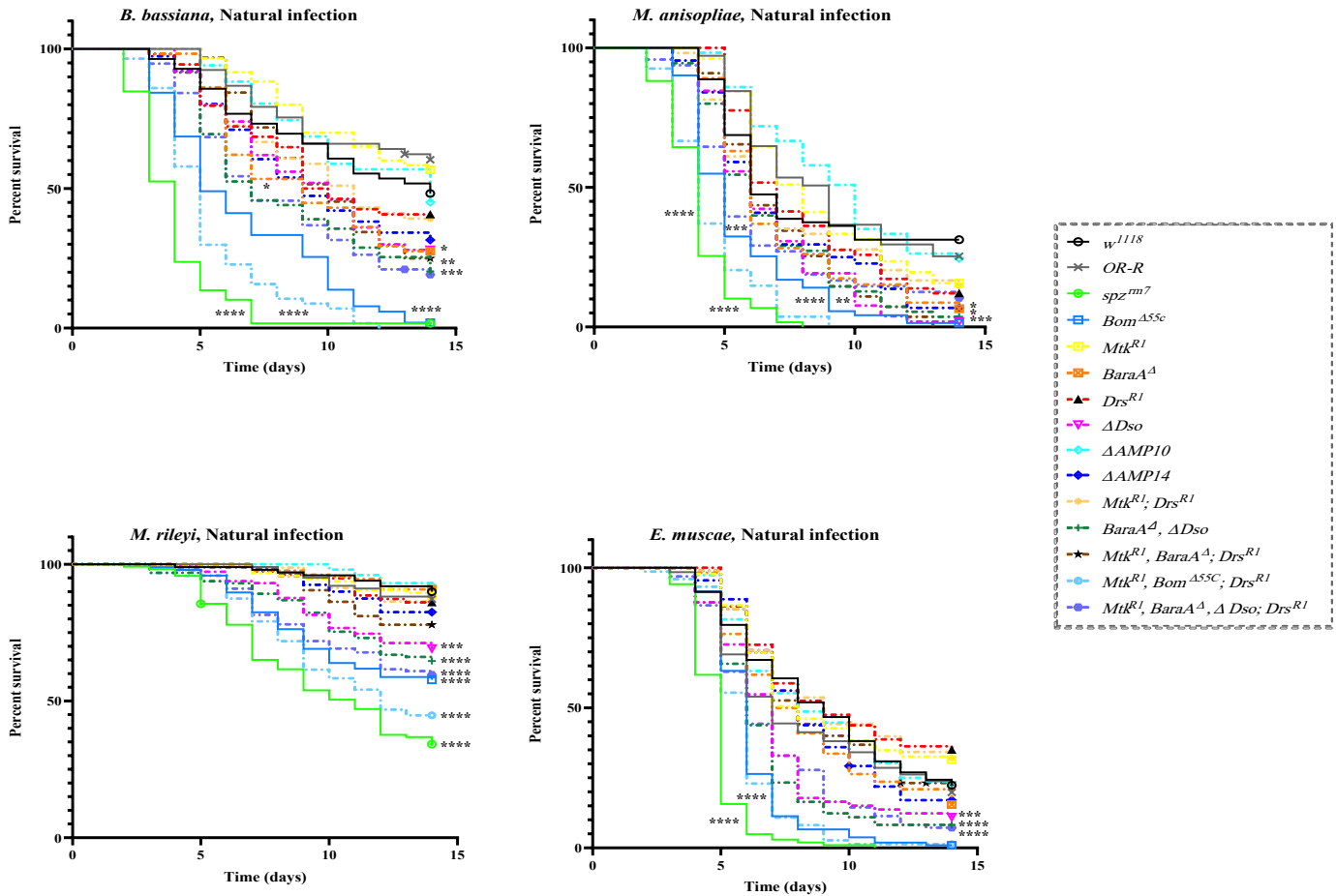
B. bassiana, Natural infection
M. anisopliae, Natural infection
M. rileyi, Natural infection
E. muscae, Natural infection
Percent survival
Time (days)
w1118
OR-R
spzrm7
BomΔ55c
MtkR1
BaraAΔ
DrsR1
ΔDso
ΔAMP10
ΔAMP14
MtkR1; DrsR1
BaraAΔ, ΔDso
MtkR1, BaraAΔ; DrsR1
MtkR1, BomΔ55C; DrsR1
MtkR1, BaraAΔ, Δ Dso; DrsR1

Figure S9

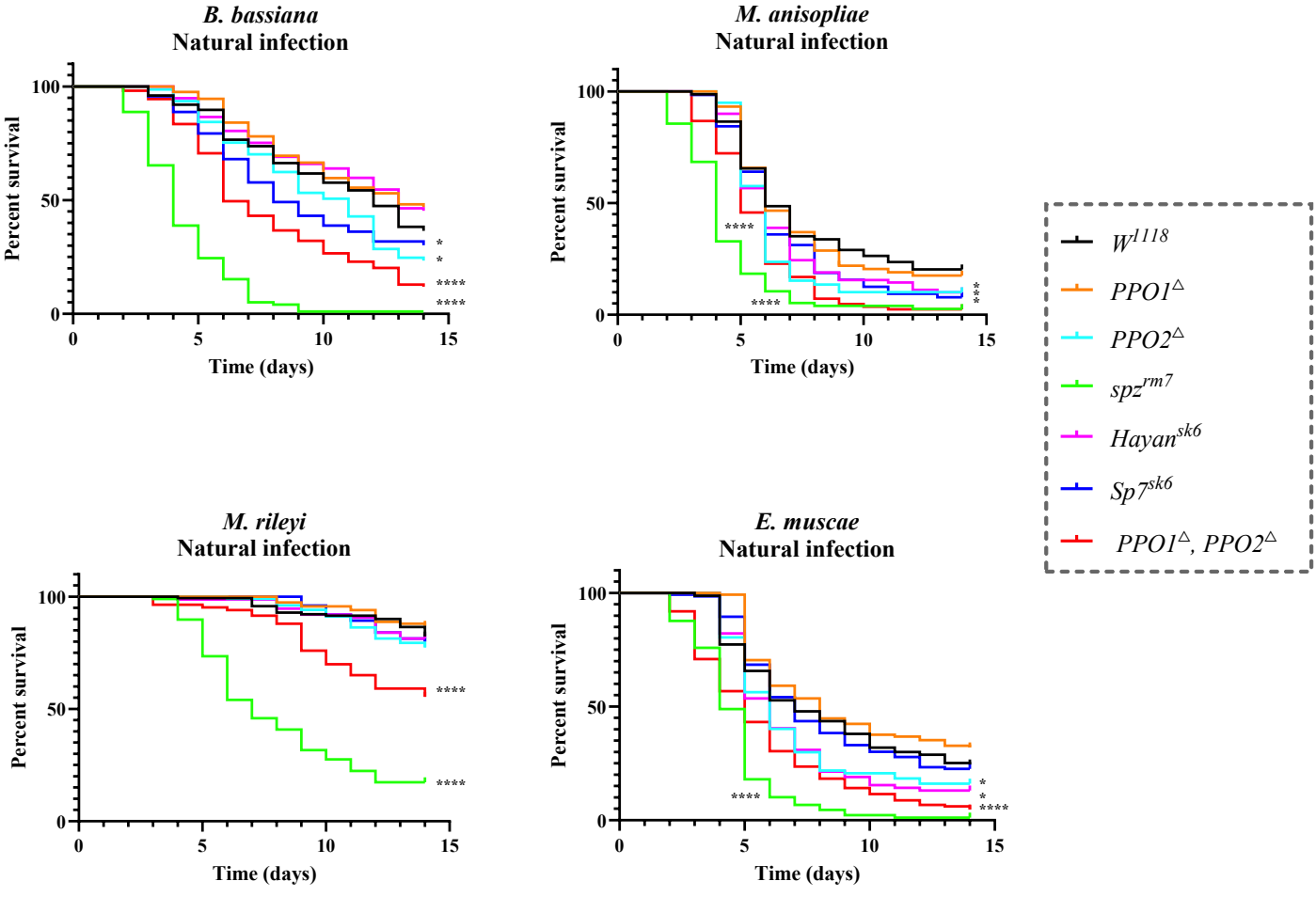
B. bassiana
Natural infection
M. anisopliae
Natural infection
M. rileyi
Natural infection
E. muscae
Natural infection
Percent survival
Time (days)
0
50
100
0
5
10
15
*
****
W1118
PPO1Δ
PPO2Δ
spzrm7
Hayansk6
Sp7sk6
PPO1Δ, PPO2Δ

Figure S10

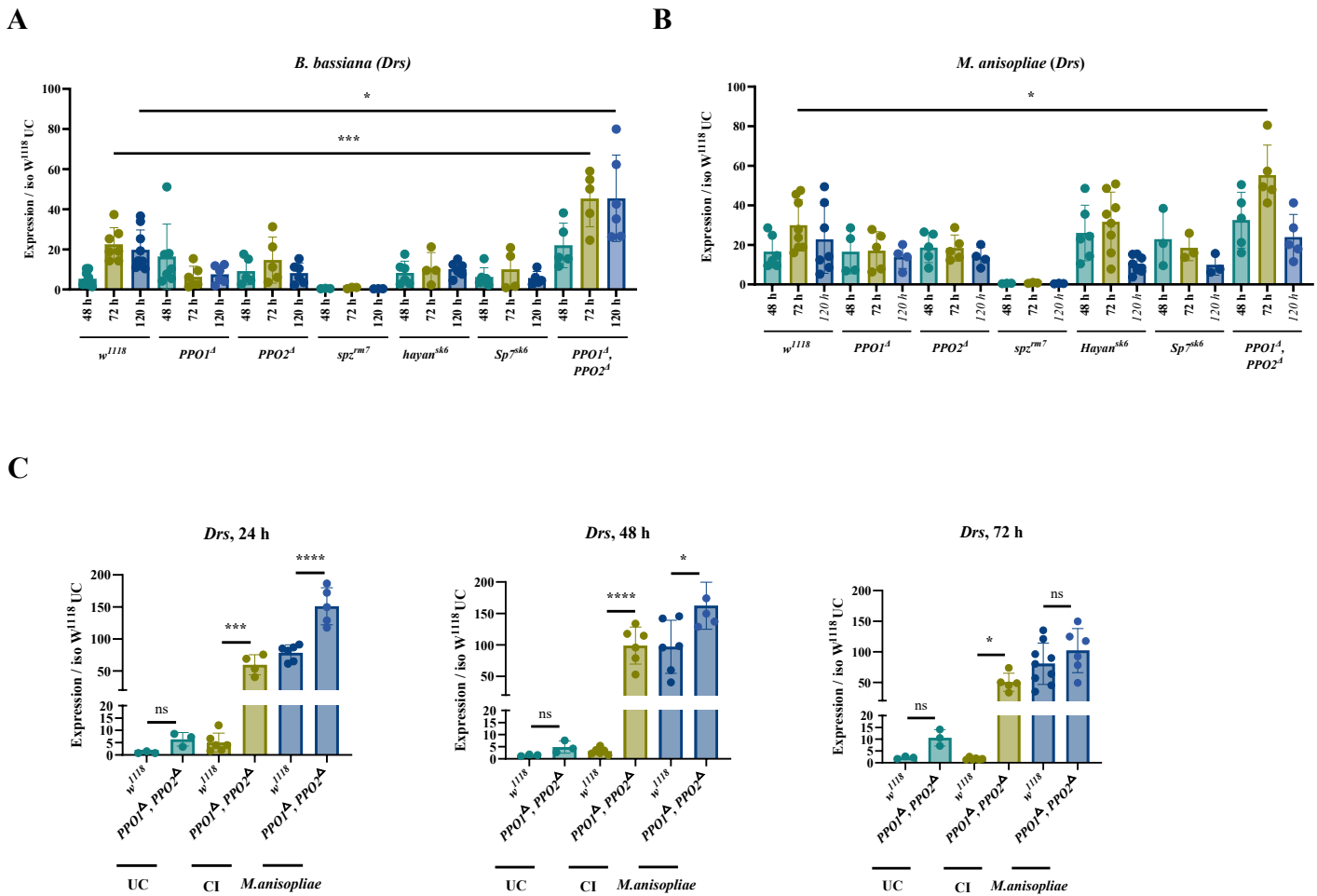
A
B. bassiana (Drs)
Expression / iso W1118 UC
*
***
48 h
72 h
120 h
w1118
PPO1Δ
PPO2Δ
spzrm7
hayanskh
Sp7sk6
PPO1Δ, PPO2Δ
B
M. anisopliae (Drs)
Hayansk6
C
Drs, 24 h
Drs, 48 h
Drs, 72 h
ns
****
UC
CI
M.anisopliae

Table S1 List of wild-type and mutant flies used in this study.

***Drosophila* lines**	**Source**	**Abbrevation**
iso; PPO1$^{\Delta}$; iso	Binggeli et al., 2014	*PPO1$^{\Delta}$*
iso; PPO2$^{\Delta}$; iso	Binggeli et al., 2014	*PPO2$^{\Delta}$*
iso; PPO1$^{\Delta}$, PPO2$^{\Delta}$; iso	Binggeli et al., 2014	*PPO1$^{\Delta}$, PPO2$^{\Delta}$*
iso; iso; Rel^{E20}	Hedengren et al., 1999	*Rel^{E20}*
iso; iso; spz^{rm7}	Lemaitre et al., 1996	*spz^{rm7}*
+; Nim C1^{1}; Eater^{1}	Melcarne et al., 2019	*Nim C1^{1}; Eater^{1}*
iso (Hayan-psh)^{Def}; NimC1^{1}; Eater1, Relish^{E20}	Ryckebusch et al., 2025	*ΔITPM*
Hayan^{SK6}; iso; iso	Duzic et al., 2019	*Hayan^{SK6}*
psh^{SK1}; iso; iso	Duzic et al., 2019	*psh^{SK1}*
Hayan-psh^{Def}; iso; iso	Duzic et al., 2019	*Hayan-psh^{Def}*
+; +; GNBP3Δ40/TM6B	Gottar et al., 2006	*GNBP3^{hades}*
iso; iso; GNBP3Δ	Lu et al., 2024	*GNBP3$^{\Delta}$*
iso; GNBP like 3Δ; iso	Lu et al., 2024	*GL3$^{\Delta}$*
iso; GNBP like 3Δ;GNBP3Δ	Lu et al., 2024	*G3$^{\Delta}$;GL3$^{\Delta}$*
w[1118];Df(3L)ED4421,P{w[+mW.ScerFRT.hs3]	BDSC#8066	*ED4421^{Def}*
iso; iso; Sp7^{SK6}	Duzic et al., 2019	*Sp7^{SK6}*
iso; iso; modSP^{1}	Buchon et al., 2009	*modSP^{1}*
Psh^{1}; iso; modSP^{1}	Buchon et al., 2009	*psh^{1};; modSP^{1}*
iso; Mtk^{R1}; iso	Hanson et al., 2019	*Mtk^{R1}*
iso; iso; Drs^{R1}	Hanson et al., 2019	*Drs^{R1}*
iso; Bom[Δ55C-289]; iso	Clemmons et al., 2015	*Bom$^{\Delta 55C}$*
iso; BaraAΔ{dsRed}; iso	Hanson et al., 2021	*BaraA$^{\Delta}$*
iso; ΔAMP10	Caboni et al., 2022	*ΔAMP10*
iso; ΔAMP14	Caboni et al., 2022	*ΔAMP14*
iso; ΔDaisho 1,2; iso	Cohen et al., 2020	*ΔDso*
iso; Mtk^{R1}; Drs^{R1}	Hanson et al., 2021	*Mtk^{R1}; Drs^{R1}*
iso; BaraA^{SW1}, ΔDso; iso	Bruno Lemaitre	*BaraA$^{\Delta}$, ΔDso*
iso; Mtk^{R1}, BaraA^{SW1}; DrsR1	Bruno Lemaitre	*Mtk^{R1},BaraA$^{\Delta}$; Drs^{R1}*
iso; Mtk^{R1}, BaraA^{SW1}, ΔDso; DrsR1	Bruno Lemaitre	*Mtk^{R1},BaraA$^{\Delta}$,ΔDso; Drs^{R1}*

iso; Mtk^{R1}, Bom$^{\Delta 55C}$; Drs^{R1}	Bruno Lemaitre	*Mtk^{R1}, Bom$^{\Delta 55C}$; Drs^{R1}*
w;; Hml^{P2A}-GAL4	Stephenson et al., 2022	*Hml^{P2A}-GAL4*
w;; UAS-CaMPARI2	Moeyaert et al., 2018	*UAS-CaMPARI2*
w; Hml Δ GAL4,UAS GFP;	Defaye et al., 2009	*Hml GAL4,UAS GFP*
w;UAS-Bax;	Gaumer et al., 2000	*UAS Bax*

Table S2 Primers used in this study.

Genes	Primers	Primer sequencs (5'-3')	Application	Source
Fly GNBP3	G3-F	TGGCGTTCAGGGGTATGAAG	Identify GNBP3 mutant	Lemaitre lab
	G3-R	CGTCTTCGCGATAACCCAGT		
Fly *Drs*	Drs_F	CGTGAGAACCTTTTCCAATATGAT	RT-PCR/qPCR	Lemaitre lab
	Drs_R	TCCCAGGACCACCAGCAT		
Fly *BomBc3*	BomBc3_F	CTGATCGGCGCTCATCCCAG	RT-PCR/qPCR	Lemaitre lab
	BomBc3_R	GGGATGAGGAGAAGCTGCGG		
Fly *Rp49*	Rp49_F	GCCGCTTCAAGGGACAGTATCTG	RT-PCR/qPCR	Lemaitre lab
	Rp49_R	AAACGCGGTTCTGCATGAG		
B. bassiana 18S rRNA	Bbas_18S_F	CGGGTAACGGAGGGTTAGG	Detection of fungal load	Hasan et al., 2021
	Bbas_18S_R	AGTACACGCGGTGAGGCGG		
Fly *actin*	Act-F	GCCAACCGTGAGAAGATGA	Detection of fungal load	Shang et al., 2023
	Act-R	GGTGGTGAAAGAGTAACCGC		
M. anisopliae Rpl32	Rpl-F	ATCGGTTTCGGGTCCAAC		
	Rpl-R	ATTCGCTTTCGGGAGGAG		
E. muscae 18SrRNA	Emus_18S_F	CGGGTGACGGGGAATAAGG	Detection of fungal load	Lemaitre lab
	Emus_18S_R	GCCAAGAACTGAAACTAACCC		